1964

Conduction characteristics of tantalum oxide films

Lyle Dean Feisel
Iowa State University

CONDUCTION CHARACTERISTICS OF TANTALUM OXIDE FILMS

by

Lyle Deán Feisel

A Dissertation Submitted to the

Graduate Faculty in Partial Fulfillment of

The Requirements for the Degree of

DOCTOR OF PHILOSOPHY

Major Subject: Electrical Engineering

Approved:

Signature was redacted for privacy.

In Charge of Major Work

Signature was redacted for privacy.

Head of Major Department

Signature was redacted for privacy.

Dean of Graduate College

Iowa State University
Of Science and Technology
Ames, Iowa

1964

TABLE OF CONTENTS

INTRODUCTION

Until very recently, the most desirable property of an electrical insulator was its ability to not conduct an electrical current. To most engineers and scientists this property is still technologically the most useful and studies continue in an effort to improve the insulating properties of materials. However, recent advances in thin film technology have uncovered the fact that when electric field intensities are high enough in a sufficiently thin insulator the current densities that are observed are considerable. In many cases, this conduction process exhibits some extremely interesting phenomena. Largely as a result of the advent of microelectronics, studies in the area of thin insulator behavior are accelerating with the goal of better understanding these phenomena. As a step toward achievement of this goal, these pages report some observations on the conduction characteristics of tantalum oxide films and attempt to relate these observations to some of the questions surrounding the theory of conduction through insulating films.

Probably the most fundamental question which is yet to be resolved is that of the mechanism of conduction through the insulating film and the nature of the interface between the film and the conducting electrodes. Basically, the question is whether Schottky emission, i.e., emission of electrons over the top of a potential barrier, or tunnel emission, i.e., tunnelling of electrons through a potential barrier is the dominant conduction mechanism. Evidence cited herein indicates that in the films studies a modified form of Schottky emission is dominant, if not solely responsible for conduction.

The modification applied to Schottky's work is necessitated by the observation that experimental volt-ampere characteristics follow Schottky's predictions if one adjusts the dielectric constant term in Schottky's equation. A hypothesis is advanced in these pages which interprets this dielectric constant, not as a ratio of electric flux density to electric field intensity, but as a measure of the degree of abruptness of the metal-insulator interface. The model thereby established is one whose effective dielectric constant is a function of the spatial distribution of ions at the interface. Migration of these ions under an applied field is proposed as an explanation of several observed peculiarities in the conduction characteristics.

The volt-ampere characteristics of many of the cells studied experimentally exhibited a negative resistance region. Certainly this is one of the most interesting phenomena observed in these devices and, at least potentially, one of the most useful. The writer's attempts to fabricate a stable, long-lived device were unsuccessful but sufficient data were obtained to allow a partial analysis of the phenomenon in the light of the modified Schottky emission model.

When one of the metal electrodes adjoining the insulator is made sufficiently thin, electrons moving through the insulator are able to penetrate the electrode and be emitted into the space beyond. Once again, cell instabilities hampered this investigation but a number of general comments are made and a partial energy spectrum of the emitted electrons is presented.

CELL FABRICATION

The cells used in this investigation consisted of a metal-metal oxide-metal sandwich about 1 to 2 square mm in area. Since the metal of prime interest is tantalum, fabrication of a tantalum pentoxide cell will be described in detail and any variations from this process will be noted.

Difficulty in depositing tantalum through a metal mask by the sputtering process necessitated the use of a multi-step process. First, aluminum was vacuum deposited on 1 by 3 inch glass microscope slides in a pattern which was the exact negative of the final tantalum pattern desired. This aluminum was about 2000 angstroms in thickness. Second, tantalum was deposited on the slide to a thickness of 2400-2500 angstroms using the sputtering process.[a] Third, the aluminum was etched away using 20% NaOH. This removal of the aluminum undercut the tantalum which was not in direct contact with glass, thereby leaving tantalum deposited in the desired pattern.

The completed slide had eleven parallel tantalum strips approximately one mm wide and 3/4 inch long extending from one edge of the slide. These strips were separated by a distance of 3/8 inch.

To facilitate electrical connection in the anodizing process, small wires were attached to the tantalum strips using conducting silver paste. Resistance of contacts made in this manner was in the order of a few tenths of ohms and was considered to be negligible.

Formation of the film of tantalum pentoxide (Ta_2O_5) was accomplished using a standard process of anodization. A 1% solution of phosphoric acid

---

[a]Tantalum deposition was carried out through the courtesy of the Microelectronics Laboratory of Collins Radio Company, Cedar Rapids, Iowa.

(H_3PO_4) was used as the electrolyte. Anodizing voltage was furnished by a variable, regulated voltage, DC supply.

In the initial stages of the anodizing process the anodizing voltage was manually increased at a rate such that the anodizing current remained nearly constant at about 10 ma/cm^2. After the desired anodizing voltage was reached, twenty additional minutes was allowed for the process to reach completion. At the end of this time the anodizing current was down to 5 to 8 $\mu a/cm^2$.

Most tantalum pentoxide cells used in this investigation were anodized to 50 volts and general comments will apply to these. Certain series of cells, however, were constructed using anodizing voltages of 40, 45, 55 and 60 volts, this variation being the only essential difference in the fabrication process.

A few cells using aluminum oxide (Al_2O_3) as the insulator were fabricated. The chief differences between the processing of these cells and the processing of the tantalum pentoxide cells are a) the aluminum strips were deposited directly through a metal mask using a resistance type evaporation source, b) an anodizing potential of only 8 volts was used and c) 3% ammonium citrate was used as the electrolyte.

The factors relating oxide thickness to anodizing voltage are 15 angstrom/volt for tantalum as given by Young (1) and 13.7 angstrom/volt for aluminum as given by Kanter and Feibelman (2).

After formation of the oxide, a counter-electrode of indium and gold was deposited over the anodized ends of the metal strips. This was accomplished by affixing about 5 mg of indium and 100 mg of gold to the same evaporation filament. Evaporation then proceeded in the normal manner

with the lower melting point and higher vapor pressure of the indium causing it to be deposited before the gold.

The predicted counter-electrode thickness, based on a spherical distribution of evaporated material and a source to substrate distance of 15 cm, is about 180 angstroms. In appearance, the counter-electrode is transparent and greenish in color which is consistent with thickness of this order.

After deposition of the counter-electrode, conducting silver paste was used to attach leads to the tantalum strips. It was also painted along the edge of the counter-electrode to reduce that element's sheet resistance. A completed slide holding 11 cells is shown pictorially in Figure 1.

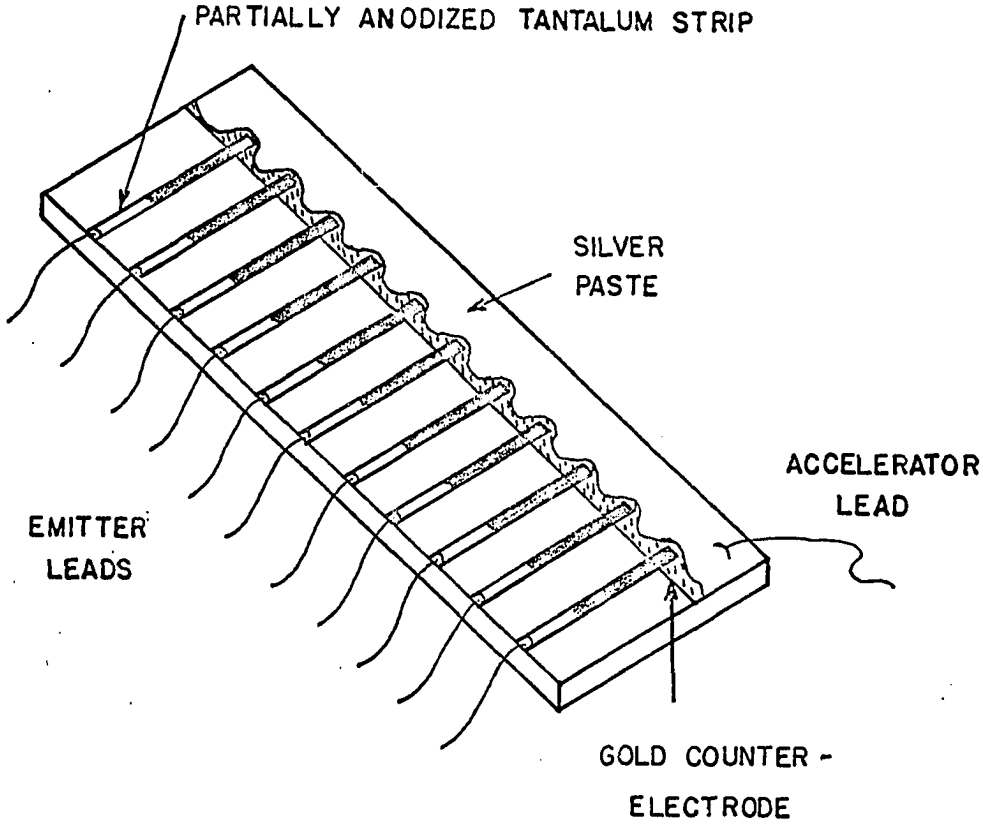

Figure 1. A representation of a microscope slide holding eleven cells showing silver paste electrode and lead attachment

TEST PROCEDURES

With very few exceptions, all cells were tested at room temperature and in a vacuum of 6 to 50 microtorr. (One microtorr = 10^{-6} mm H_g) To facilitate testing a number of cells with one pumpdown of the vacuum system, a fixture was constructed which allowed the emitter leads of all eleven cells on one slide to be connected to separate feedthrough pins. This allowed switching from one cell to another without breaking vacuum. Pins were also provided for the common accelerator lead and the collector lead.

A 1 x 3 inch glass microscope slide coated with gold on one side was mounted directly above the sample to serve as a collector during emission studies. The spacing between the cell under test and the surface of the collector was about 1 mm. The cell and collector are shown schematically in Figure 2. The thickness of all films are of necessity greatly exaggerated.

The electrical circuit used in determining conduction characteristics is shown in Figure 3. Use of the x-y recorder allowed a constant record of cell behavior to be kept, including any transient unstable behavior. The recorder was also equipped with a time base which allowed the plotting of current versus time.

A Hewlett-Packard Model 425A microvolt-ammeter was used for measuring emission current. The output of the meter amplifier was connected to the x-y recorder thereby allowing plots of emission current versus time or retarding potential. The electrical circuit used in emission studies is shown in Figure 4.

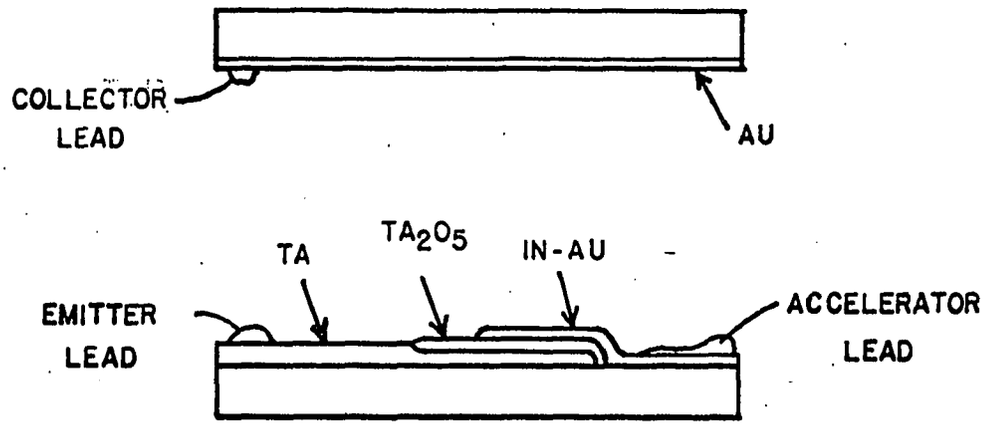

Figure 2. Arrangement of an experimental cell and collector for electron emission studies

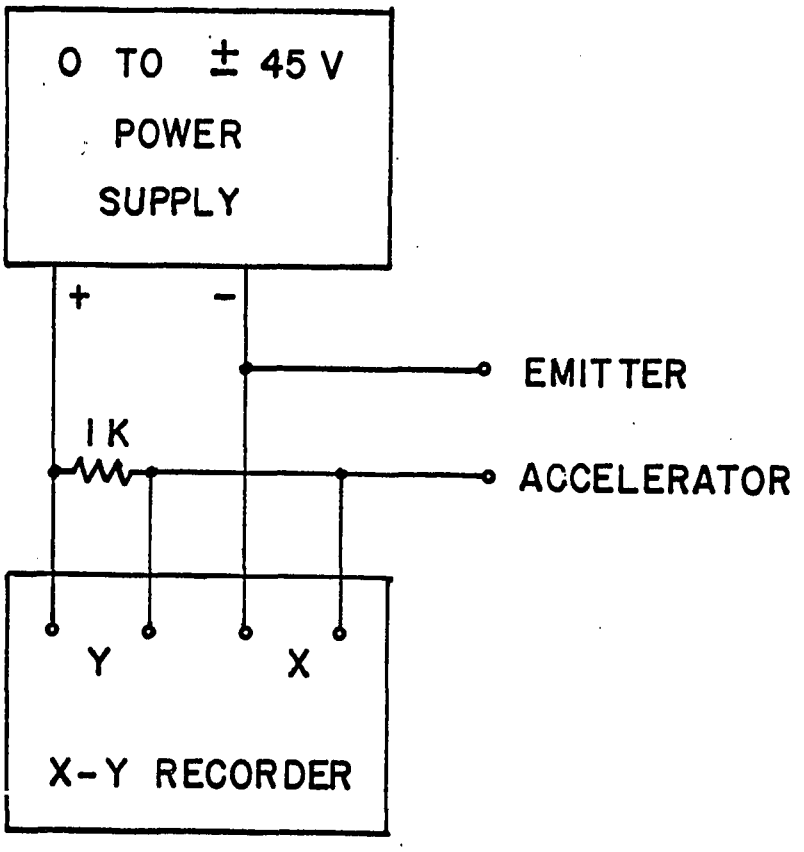

Figure 3. Circuit used in the determination of cell conduction characteristics

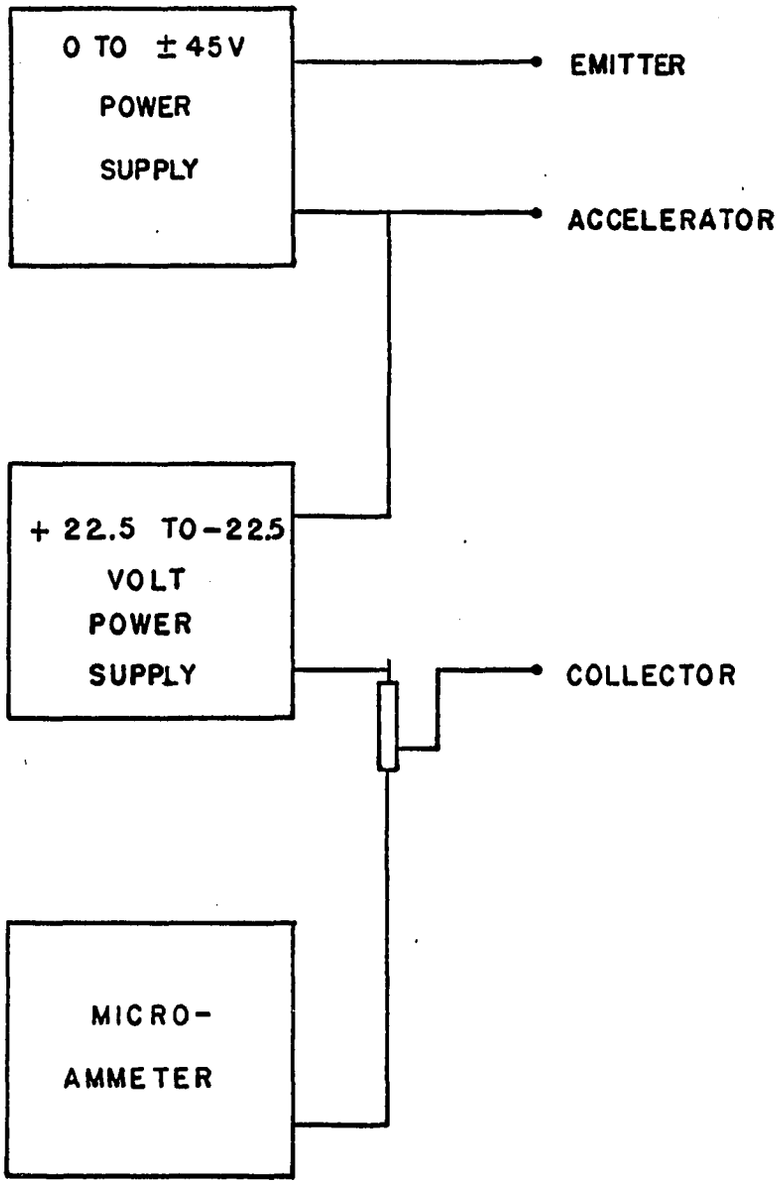

Figure 4. Circuit used in the determination of electron emission characteristics

SIMPLE CONDUCTION

Introduction

Simple conduction through thin insulating films has been treated at length by a number of authors. One of the earlier treatments is that of Bethe and Sommerfeld (3) in 1933 closely followed by an expansion by Holm and Kirschstein (4) in 1935. With the advent of thin film technology and the accompanying use of thin anodic oxide capacitors interest in this phenomenon began to intensify about 1960. In that year, Mead (5) proposed a thin film triode based on the conduction properties of thin insulators. Since then a profusion of papers, both theoretical and experimental, have appeared.

Conduction mechanisms

When the vacuum of a metal-vacuum interface is replaced with an insulator the relatively familiar concept of a work function is complicated considerably. Some authors, such as Hickmott (6) draw the new potential diagram by matching vacuum levels as shown in Figure 5a. In this manner, a barrier $\phi_{eff} = \phi_m - \chi$ is achieved where ϕ_m is the work function of the metal and χ is the electron affinity of the insulator. This model seems to ignore any matching of Fermi levels at the interface.

Extension of Schottky's model of a metal-n-type semiconductor interface yields a barrier of the type shown in Figure 5b. The barrier is still $\phi_m - \chi$ but is rather narrow if a high density of ions is assumed. This model does provide a matching of Fermi levels, but the assumption of a large ion density in the insulator is somewhat objectionable.

Figure 5. Three different models of a metal-insulator interface

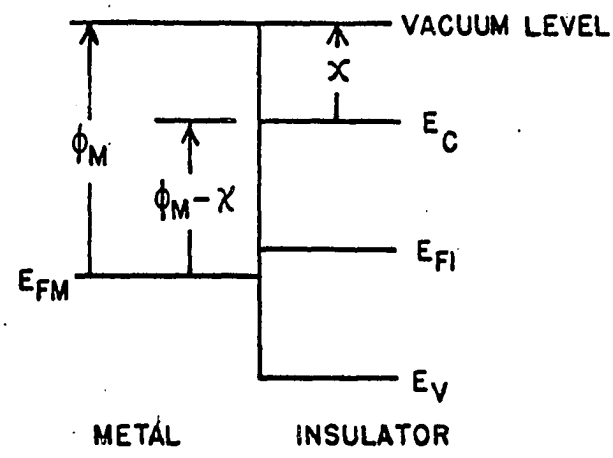
VACUUM LEVEL
χ
E_C
ϕ_M
$\phi_M - \chi$
E_{FI}
E_{FM}
E_V
METAL
INSULATOR

(A)

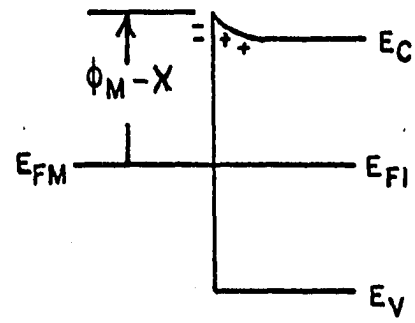
E_C
$\phi_M - \chi$
E_{FM}
E_{FI}
E_V

(B)

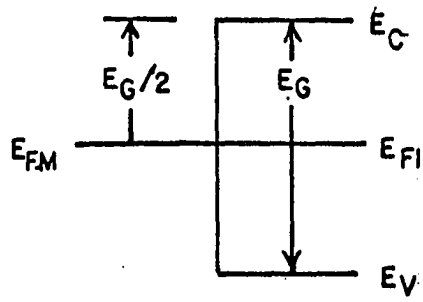
E_C
$E_G/2$
E_G
E_{FM}
E_{FI}
E_V

(C)

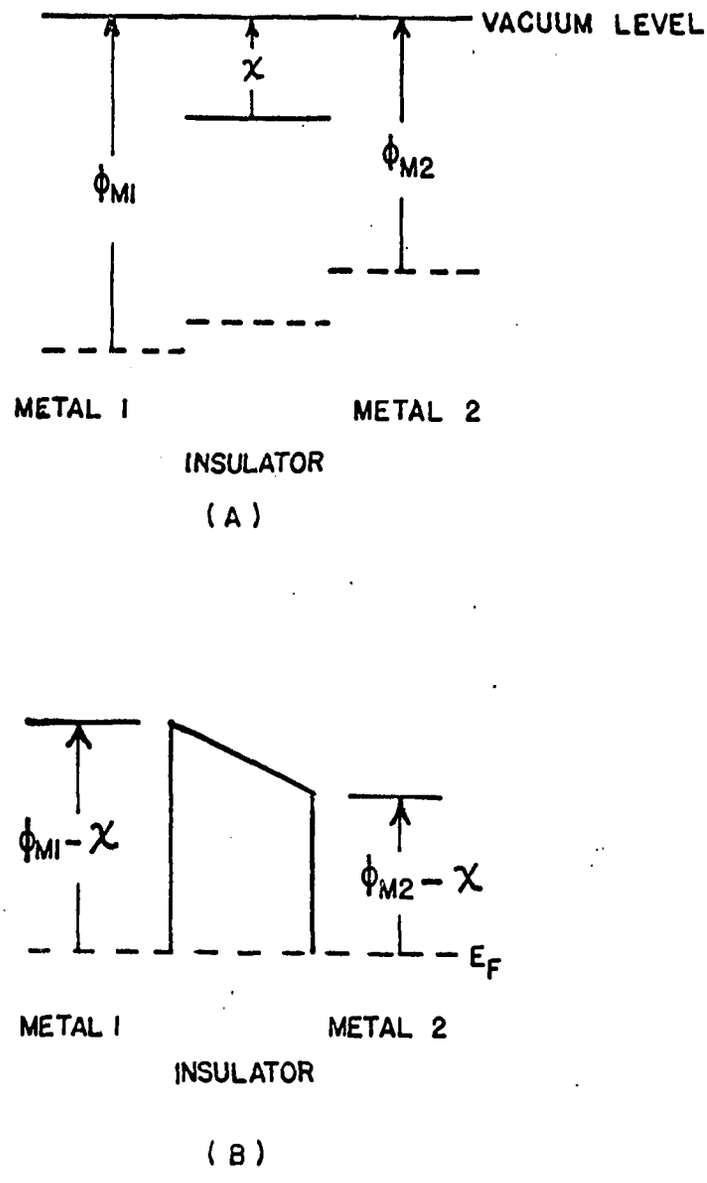

Figure 6. A metal-insulator-metal interface (a) just after contact and (b) after equilibrium has been established

A third possibility is a model based entirely upon the principle that the Fermi levels of elements in contact must be equal right at the interface. The barrier height is now independent of the work function of the metal and is equal to $E_g/2$ where E_g is the gap energy of the insulator. This independence of the metal work function is not borne out experimentally.

The model which seems the most plausible is one which provides for Fermi level matching and yet requires no ions in the insulator. This model is developed for an insulator and two dissimilar metals in Figure 6. Now the barrier is dependent upon the electron affinity of the insulator, χ, and the work functions of the metal. (7)

At any rate, some barrier to electron flow exists at any metal-insulator interface. Perhaps, if one were able to fabricate an ideal interface, this barrier could be evaluated with some degree of precision. However, in any practical interface it seems plausible to assume that the interface is actually diffuse and the barrier, while having a dependence upon both the insulator electron affinity and the metal work function cannot be simply described in these terms.

Conduction of electrons across this barrier can be accomplished by several mechanisms. These are shown schematically in Figure 7 for a biased cell.

Direct tunnelling from metal to metal (line a, Figure 7) requires a barrier less than about 100 angstroms if measurable currents are to be obtained. If one assumes that the barrier is the same thickness as the oxide layer (which is true of the simple model of Figures 5 and 7) this

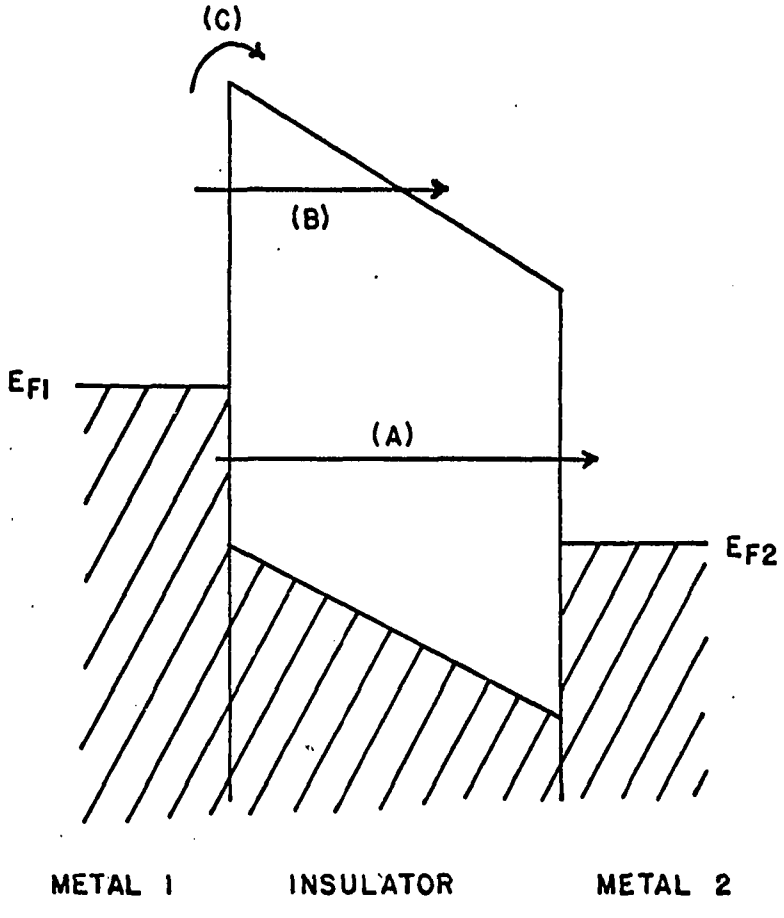

Figure 7. Idealized potential showing three mechanisms of electron conduction: (a) direct tunnelling, (b) tunnelling into the conduction band, and (c) Schottky emission

type of conduction must be ruled out in the films treated here. One may, however, hypothesize conversion of a portion of the insulator to an essential semiconductor by injection of excess electrons, thereby reducing barrier thickness.

Tunnelling from the metal to the insulator conduction band (line b, Figure 7) followed by ordinary conduction of these electrons is, under the same assumption, limited to very thin barriers.

Thermionic emission or Schottky emission of electrons into the insulator conduction band (line c, Figure 7) results from an effective lowering of the barrier by high electric field intensities. The field intensities necessary for measurable currents are on the order of 10^7 v/cm and are encountered in these experiments.

In the derivation of the Schottky effect, the potential barrier is characterized in terms of a force between an emitted electron and its equal and opposite image charge inside the metal. This yields a barrier which is smooth and depends upon the characteristics of both the metal and the insulator. (8) It is this type of barrier which will be used as the basis of hypotheses which will follow.

Data

A typical volt-ampere characteristic for a 2 square mm, 750 angstrom tantalum pentoxide cell is shown in Figure 8. This characteristic was obtained after completion of a forming process to be discussed later and was completely stable through many cycles. The In-Au electrode was positive.

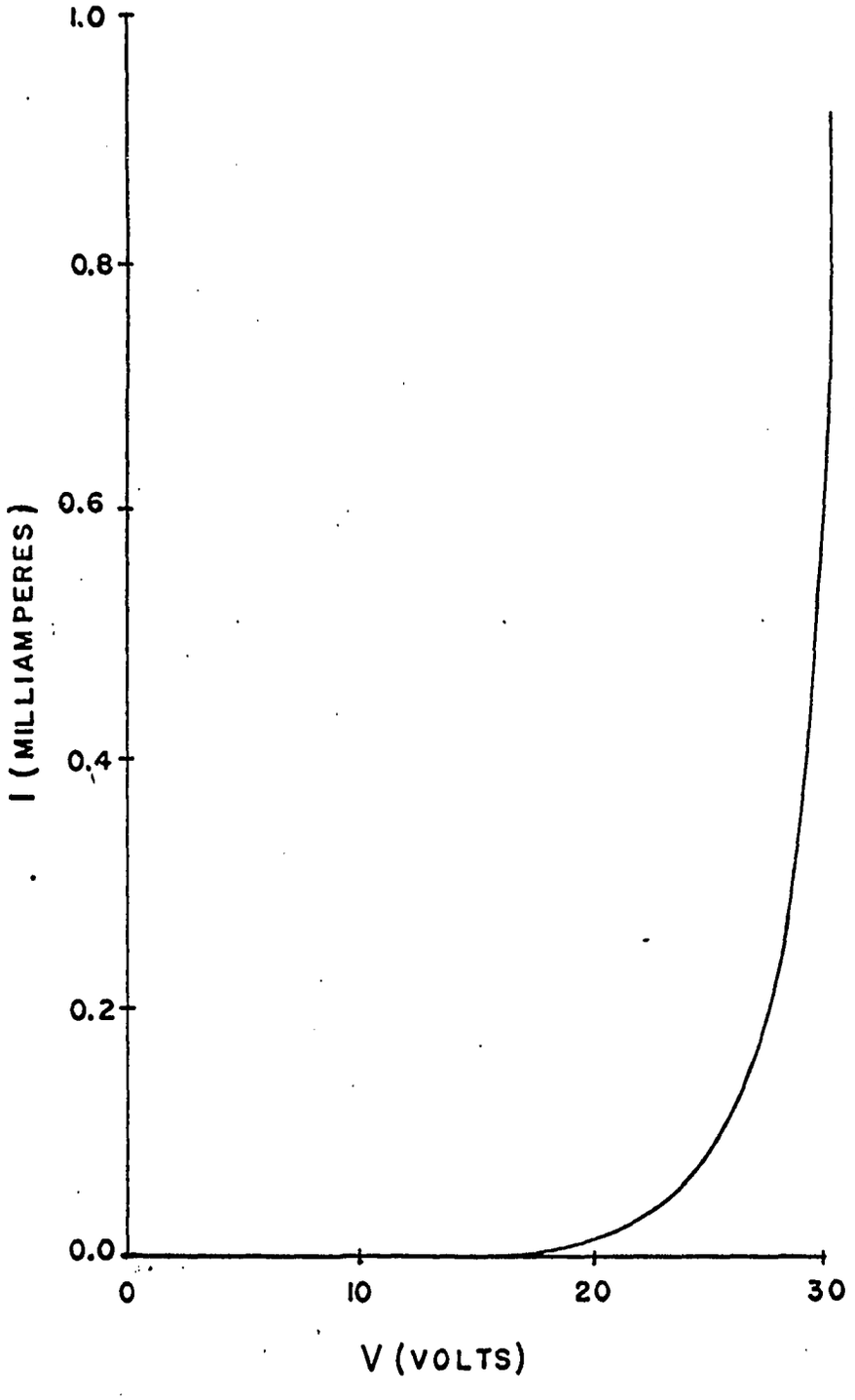

Figure 8. Typical volt-ampere characteristic of a 750 angstrom Ta_2O_5 cell.

It is immediately apparent that the conduction characteristics are governed by some exponential relationship. The exact form of this relationship may serve as a key to the type of conduction mechanism which is operative in this case.

Conduction by tunnelling is governed by the familiar Fowler-Nordheim equation,

$$I = \alpha_F \ V^2 \ \exp(-\beta_F/V) \qquad a/cm^2 \qquad (1)$$

where

$$\alpha_F = e^2 \ /8\pi \ h\phi \ a^2 \qquad (2)$$

and

$$\beta_F = 8\pi \ a(2m)^{\frac{1}{2}} \ \phi \ ^{3/2}/3he. \qquad (3)$$

In these equations, e is the electronic charge, h is Planck's constant, ϕ is the barrier height in eV, a is the barrier thickness, and m is the effective mass of the electron usually taken as equal to the rest mass. (9)

Note that if tunnelling is the dominant mechanism of conduction in a cell (i.e. if the Fowler-Nordheim equation is obeyed) a plot of log I/V^2 versus $1/V$ should yield a straight line.

Conduction by Schottky emission into an insulator is described by the relationship

$$I = \alpha_s \exp(\beta_s V^{\frac{1}{2}}) \tag{4}$$

where

$$\alpha_s = AT^2 \exp(-\phi/k\,T) \tag{5}$$

and

$$\beta_s = (1/k\,T)\,(e^3/K\epsilon_o\,a)^{\frac{1}{2}} \tag{6}$$

In these equations, A is the Richardson constant (120 $A/cm^2\ ^oC$), T is the absolute temperature, k is Boltzmann's constant, K is the dielectric constant of the insulator, and ϕ, a, and e are as previously defined.

If Schottky emission is the dominant mechanism of conduction, a plot of log I versus 1/V should yield a straight line.

Figures 9 and 10 show a Fowler-Nordheim plot and a Schottky plot, respectively, of the data of Figure 8. The Fowler-Nordheim plot shows a very good fit to a smooth curve, making any "best fit" to a straight line impossible. The Schottky plot, on the other hand, shows a very good fit to a straight line throughout the accurate range of measurement, i.e., about the knee of the volt-ampere characteristic.

Analysis of the Schottky plot indicates an effective dielectric constant of 35 and a potential barrier of 1.0 eV. The dielectric constant of 35 is in generally good agreement with that of 25 quoted by Hickmott. (6) The barrier height of 1.0 eV is quite reasonable, but absence of information on the electron affinity of Ta_2O_5 precludes any verification. However, if one assumes that the barrier height is $\phi_m - \chi$ and that the bulk

Figure 9. Fowler-Nordheim plot of the characteristic of Figure 8

Figure 10. Schottky plot of the characteristic of Figure 8

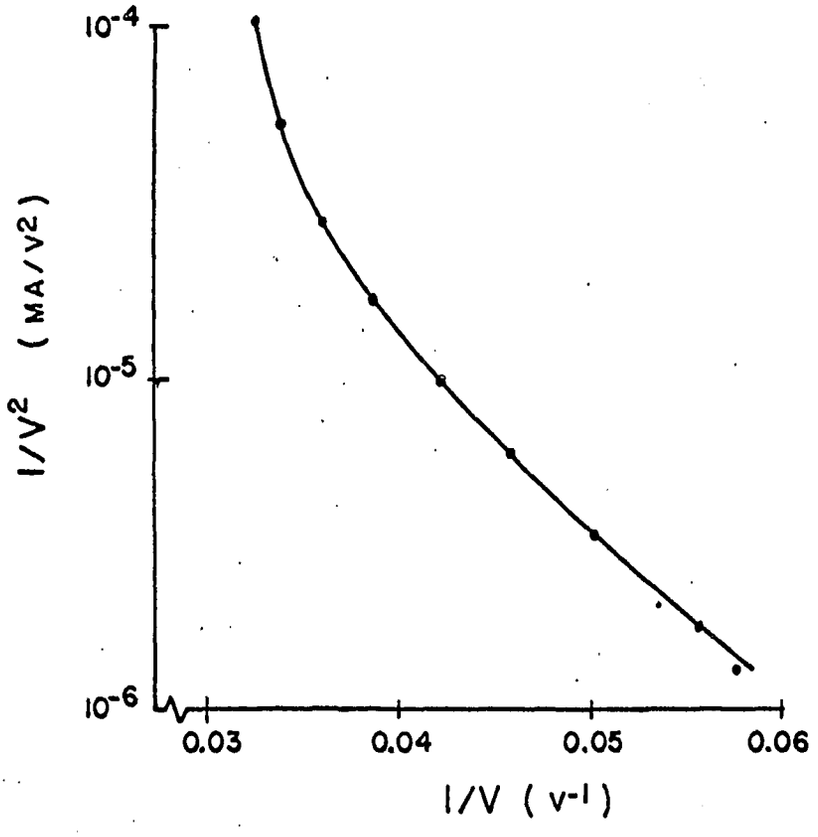
10^{-4}
10^{-5}
10^{-6}
I/V^2 (MA/V2)
0.03
0.04
0.05
0.06
I/V (v-1)

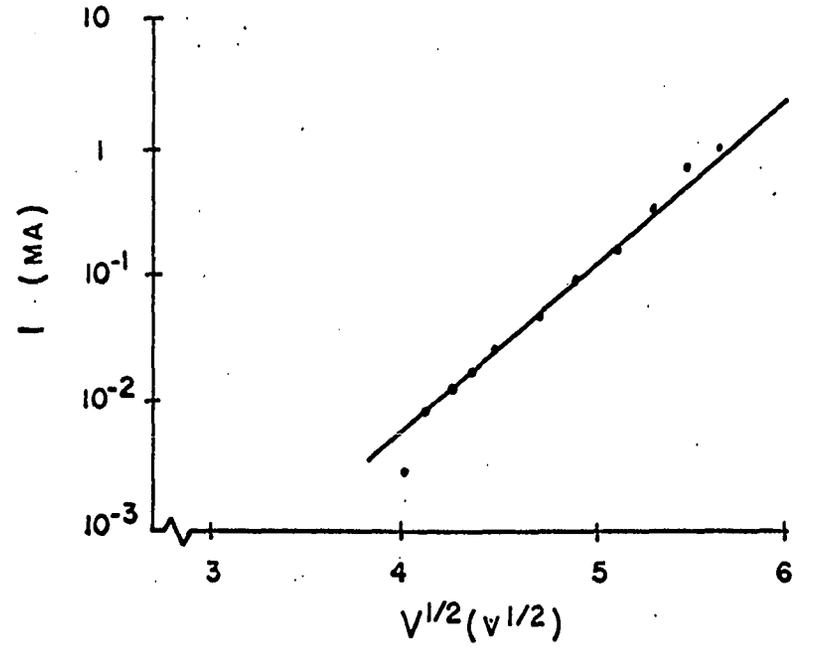
10
1
10^{-1}
10^{-2}
10^{-3}
I (MA)
3
4
5
6
$V^{1/2}$ ($v^{1/2}$)

value of 4.19 eV for the work function of Ta_2O_5 holds in this situation, an electron affinity of 3.19 eV is determined.

This evaluation of electron affinity may be somewhat questionable. Pollack and Morris (10) determined an electron affinity for Al_2O_3 of 1.58 eV by considering tunnelling through a thermally grown Al_2O_3 film. Heil, (11) by another method, determined a value of about 2 eV. Analysis of the volt-ampere characteristics of an anodically formed Al_2O_3 film by this writer by assuming Schottky emission yields a value of 2.54 eV. This same analysis yields a dielectric constant of 15, about double the value of 8 quoted by Hickmott (6). These deviations, along with an inadequate knowledge of the barrier formation mechanisms operative at the metal-insulator interface indicate that it would be unwise to say that the value of χ = 3.19 eV determined here is any better than a first approximation to the true electron affinity of Ta_2O_5. The reasonable fit of data to the Schottky plot along with recent evidence in favor of Schottky emission as the dominant mechanism of conduction in thin Ta_2O_5 films (12) indicate that the value of ϕ = 1.0 eV is a reasonable phenomenological measurement for these cells.

Voltage induced transients

When voltage is first applied to a Ta_2O_5 cell some very interesting properties are noted. These are illustrated in Figure 11. If voltage is first applied in the forward direction (i.e. In-Au positive) curve 1 of Figure 11a is established. If the voltage is not removed, the current decreases monotonically in a timewise exponential fashion to a value such that if the voltage is now decreased to zero, curve 2 is swept out. A

Figure 11. Volt-ampere characteristics of a Ta_2O_5 cell (a) before catastrophe and (b) after catastrophe

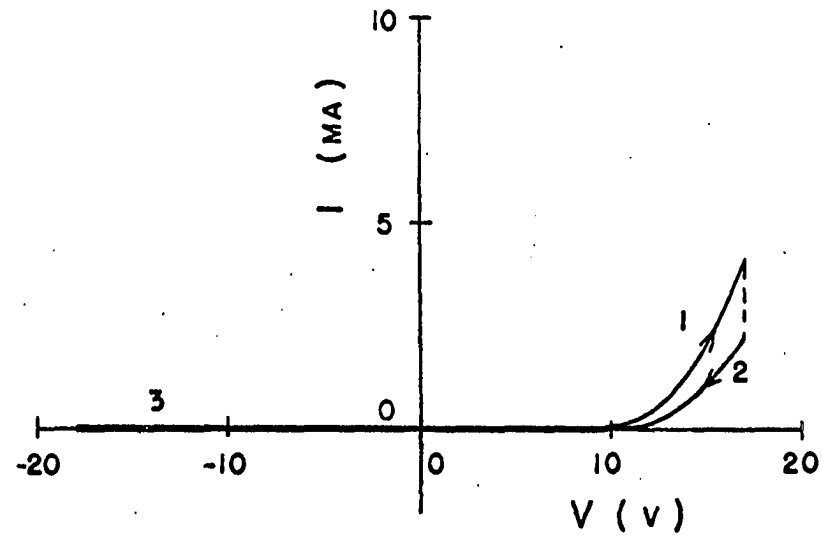

(A)

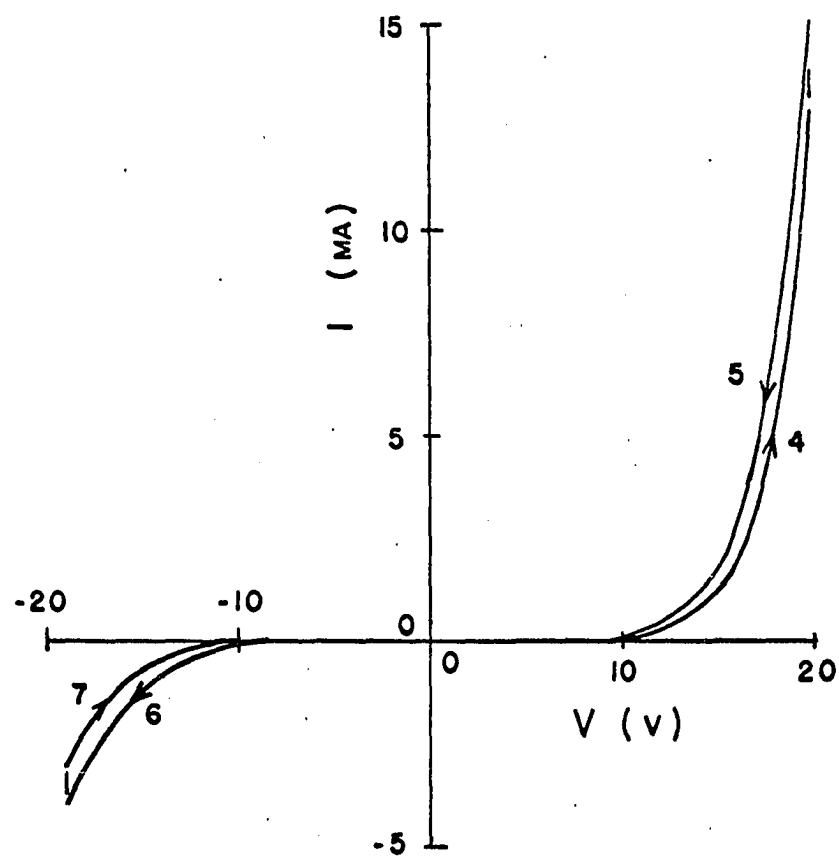

(B)

reversal of voltage shows no measurable current flow.

If voltage is now increased in the forward direction to a value greater than the maximum in Figure 11a, an irreversible catastrophe occurs at some voltage which results in a sudden increase in current at constant voltage. Now if the voltage is decreased to zero and reapplied in the forward direction, curve 4 of Figure 11b is established and if the voltage is not removed, the current increases at constant voltage. Decreasing the voltage then sweeps out curve 5.

Now if a voltage is impressed in the reverse direction, current flows and curve 6 is established. Leaving this negative voltage applied results in a slow exponential decrease in current at constant voltage such that removal of the voltage sweeps out curve 7.

The sequence of events may be summarized as follows:

1. Forward voltage - current decreases
2. Reverse voltage - no current
3. Catastrophe occurs
4. Forward voltage - current increases
5. Reverse voltage - current decreases

Note that after the catastrophe the cell behaves under reverse voltage just as it did under forward voltage before the catastrophe occurred.

The behavior summarized in items 4 and 5 above (i.e., after catastrophe) was first reported by Fisher and Giaever (9) in Al_2O_3 cells. Further observations were made by Pollack and Morris, again employing the same material. Neither report the presence of any catastrophic change in behavior.

The time constants on all current changes are on the order of 20 or 30 seconds. The forward current is then of the form

$$I = I_{final} - \Delta I\, e^{-t/\tau} \tag{7}$$

In some cases, if the cell voltage is not removed after the second term in the above equation becomes insignificant, the current starts to rise again, now of the form

$$I = I_{final}\, e^{t/T} \tag{8}$$

It is apparent that if allowed to continue in this manner the cell is ultimately destroyed. The time constant, T, on this latter process is on the order of several minutes and, as such, appears to be basically thermal in nature. It is therefore felt that this process is not directly related to the initial increase in current noted above.

Analysis

Three means of explaining this phenomenon are suggested:

1. Thermal effects
2. Change of trap occupancy
3. Ion migration

The first, thermal effects, can probably be eliminated for two reasons. First, the thermal time constants observed are long relative to the time constants involved in the voltage induced transients. Second, it would appear that thermal effects would have a similar effect in both the forward and reverse directions.

Changes in the occupancy of traps in the insulator would certainly change the barrier parameters and hence change the current. The ability of Fisher and Giaever to "quench in" a given state of the cell (i.e., reduce the temperature of a cell while it is operating in a given state and thereby retain that state) indicates, however, that trapping is not the mechanism sought since trap occupancy is a function of temperature (9).

In the formation of a surface oxide by either thermal or anodic oxidation, the migration of ions is certainly involved. If one assumes that oxygen ions are the mobile elements in the anodic process the factor of 15 angstroms/volt of anodizing potential indicates that an oxygen ion will migrate through Ta_2O_5 under a field greater than about 6×10^6 v/cm. Certainly these field intensities are present, at least locally, in an operating cell so it seems reasonable to assume that some migration will occur. When ions migrate, variations from stoichiometry will occur and it is apparent that concurrent changes in barrier parameters will result. Wide variations in the conductivity of TiO_2 result from very modest deviations from stoichiometry and it seems reasonable to assume that similar effects are present in Ta_2O_5 which might give rise to the following situation.

At the interface between the Ta electrode and the Ta_2O_5, some gradation of oxygen concentration must occur. The gradation is probably on the order of that shown in Figure 12a. If a forward voltage is applied to the cell such that a point in the insulator is positive with respect to the Ta, oxygen ions will tend to migrate toward the insulator. This tendency will cause the graded interface to become less diffuse (i.e.

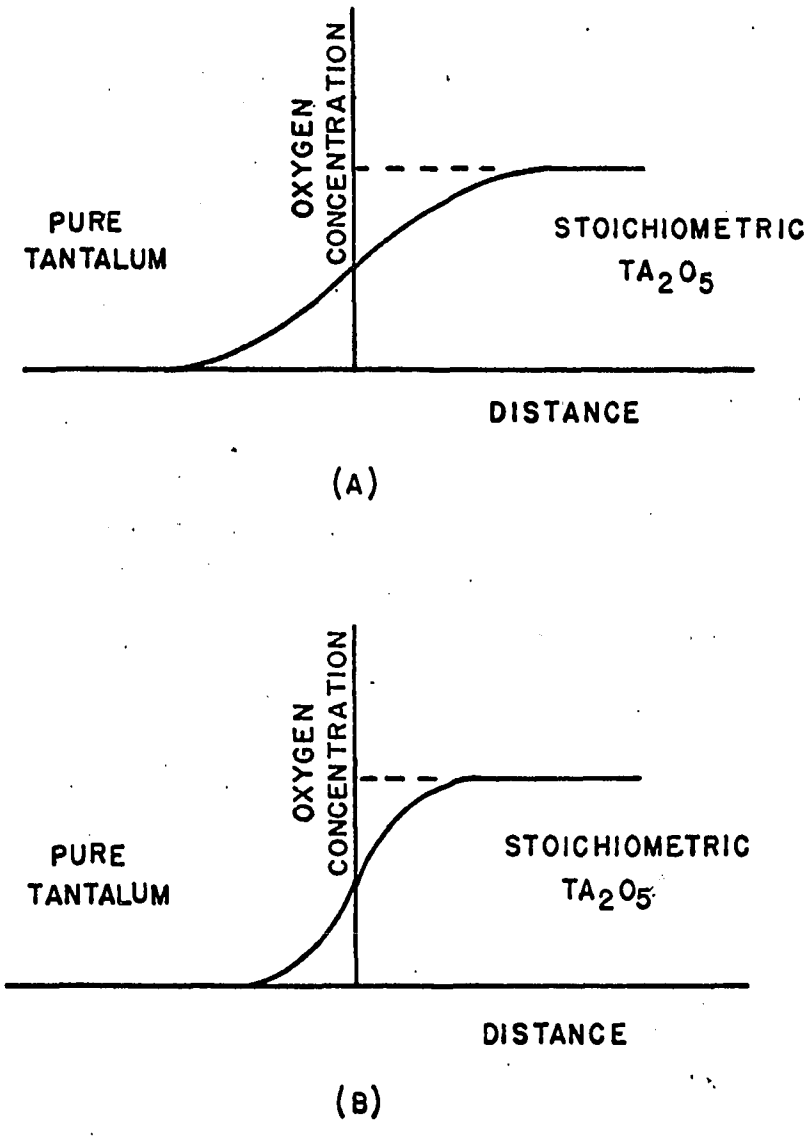

Figure 12. Ta -Ta_2O_5 interface with (a) no voltage applied and (b) voltage applied

closer to a discrete interface) as shown in Figure 12b. Certainly this will cause an increase in the slope of the potential diagram. It will now be shown that this increase in slope can be interpreted as a change in effective dielectric constant and that its effect on conduction current can be significant.

In the derivation of the equation governing Schottky emission, a potential barrier is expressed in terms of a force on an emitted electron due to an image charge inside the metal. If this is done, the barrier potential, $\phi(x)$, is given by

$$\phi(x) = \frac{e}{16 \pi K \epsilon_o x} \tag{9}$$

with zero potential being taken as the bottom of the conduction band of the medium into which emission is taking place. Figure 13 shows two Schottky barriers having different values of dielectric constant, K.

The effect of this change in K upon the number of electrons which pass over the barrier can be seen in Equation 6.

$$\beta_s = \frac{1}{kT} \quad (e^3/K \epsilon_o a)^{\frac{1}{2}} \tag{6}$$

An increase in K causes a decrease in β_s and a corresponding decrease in current at a given voltage and vice versa.

If one now considers the potential barriers corresponding to the two oxygen distributions of Figure 12, one sees that the more diffuse interface (Figure 12a) corresponds to the image potential model having the lower K (Figure 13a). It follows, then, that if an applied field makes the

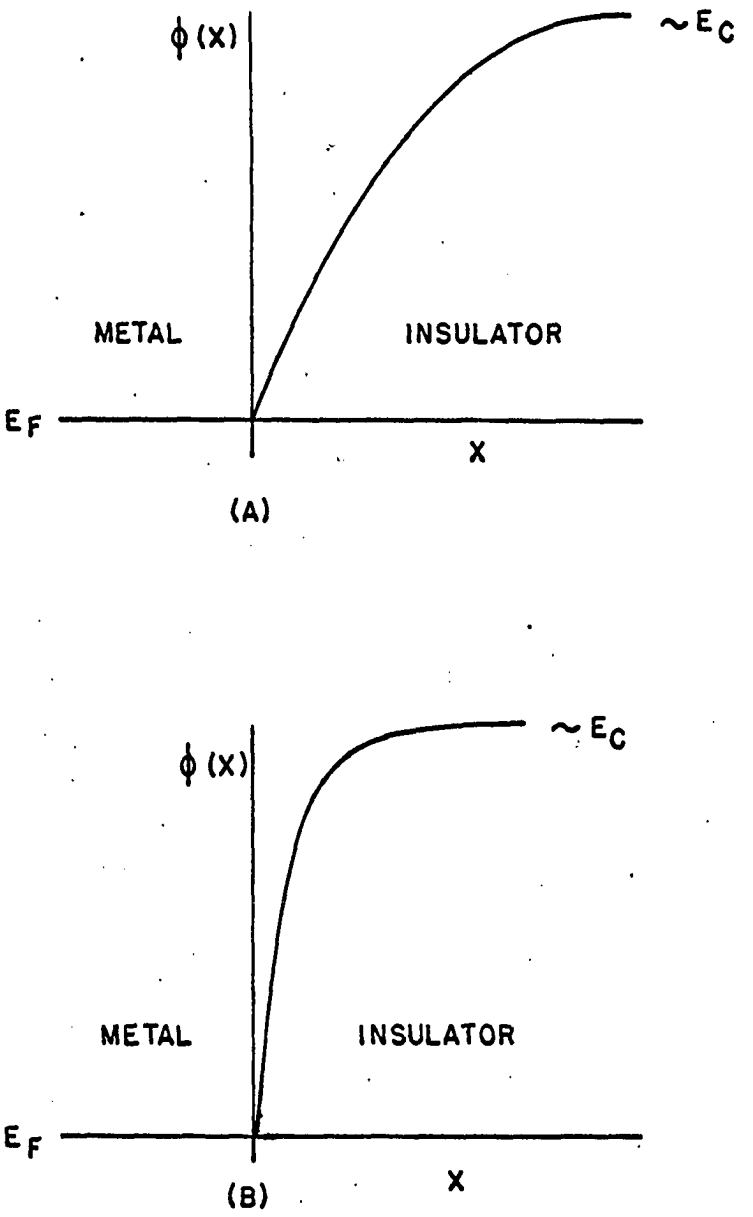

Figure 13. Schottky barrier at a metal-insulator interface: (a) low dielectric constant and (b) high dielectric constant

interface less diffuse through ion migration the insulator has a higher effective dielectric constant which results in a decrease in current. This is indeed the case prior to the catastrophe.

One feels that the width of the diffuse area of the interface can only be on the order of a few angstroms and this is in good agreement with the image potential model of Equation 9. A simple calculation based on that equation reveals that the image potential is within 0.1 volts of its minimum value at x = 7.2 angstroms for a K of 5 and at x = 1.5 angstroms for a K of 25. It seems reasonable, then, that a diffuse interface may have a width in this range and that a change in degree of diffusion of the interface may be characterized by a change in effective dielectric constant, K_{eff}.

The argument just presented which predicts a forward current decrease due to ion migration is predicated on the assumption that oxygen concentration through the bulk of the insulator and at the opposing interface does not change with a change in the degree of diffusion at the interface in question. If the interface of the In-Au electrode and the Ta_2O_5 was only very slightly diffuse this would indeed be true. The method of depositing the counter-electrode indicates that this interface is probably quite abrupt, at least initially. This also agrees with the observed fact that no current flow takes place in the reverse direction until some irreversible change takes place in the structure of the cell.

The exact nature of the physical change that takes place at the time of the conduction catastrophe is difficult to assess. Since it results in the cell being able to conduct current in the reverse direction with-

out radically changing the forward characteristics, the major physical change undoubtedly takes place at the interface of the Ta_2O_5 and the In-Au counter-electrode. And since the catastrophe occurs while the cell is biased in the forward direction and drawing current, the effect is probably due to thermal action.

Let us assume that, regardless of what physical change takes place at the interface, the result of that change is to allow oxygen ions to enter the counter-electrode. This would create a diffuse interface and allow the reverse conduction which is observed. It now remains to determine what type of voltage induced transients will result from this new situation.

The only effect that the newly attained ability of the counter-electrode to accept oxygen ions will have upon the Ta-Ta_2O_5 interface is that now oxygen ions may move away from that interface toward the counter-electrode. Figure 14 shows that this ability of the ions to move away from the Ta has a quite significant effect upon the value of K_{eff} at the interface. Curve a shows the oxygen concentration in the interface with no voltage applied to the cell. As before, application of voltage results in migration of the oxygen ions so that if no ions are allowed to pass the plane P, curve b results and K_{eff} increases. Note that this restriction on the migration of the ions demands that the area under curve a must equal that under curve b. If this restriction on ion migration is now lifted by the ability of the counter-electrode to accept oxygen, the concentration of oxygen will approach that shown in curve c. This creates a more diffuse interface resulting in a decrease in K_{eff} and a corresponding increase in current. As noted earlier, this is indeed what is

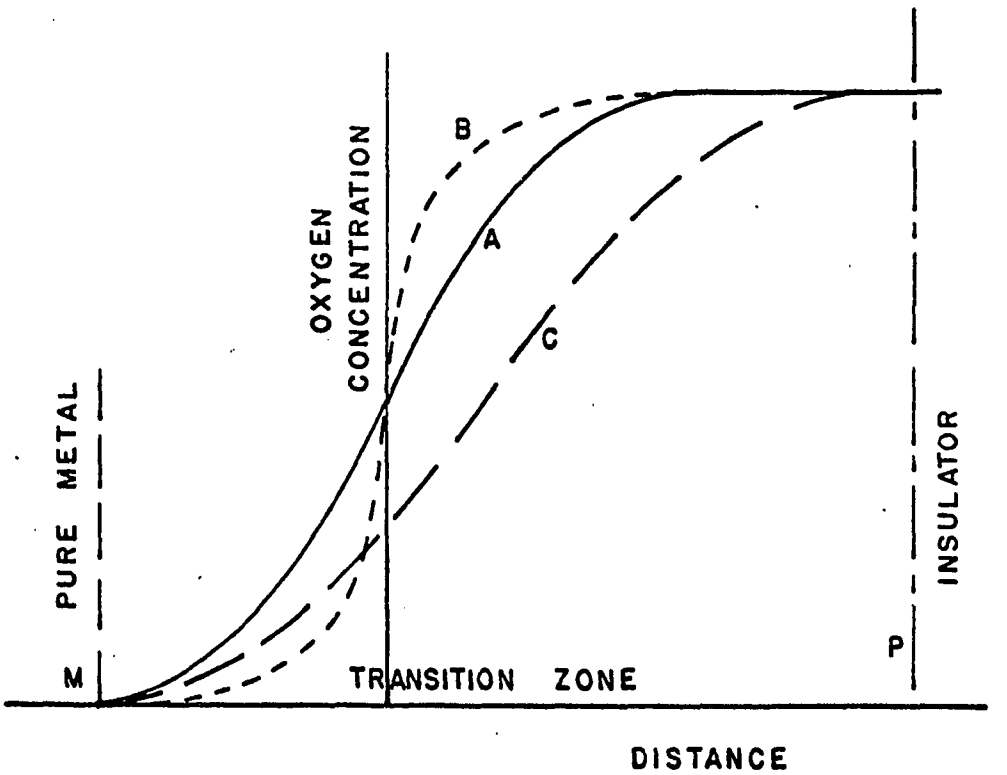

Figure 14. Oxygen concentration at a metal-metal oxide interface: (a) with no field applied, (b) with field applied and oxygen unable to cross the plane P, and (c) with field applied and oxygen permitted to cross the plane P

observed after the catastrophe.

An important point to note is that for curves b and c to result from the situations described, point m, the edge of the pure metal, must remain fixed. That this is indeed the case is evident from the fact that the slope of the barrier and hence the electric field intensity must go to zero as the metal (i.e. point m) is approached. With no field at this point, there will be no force applied to the oxygen ions and no migration will occur.

The effect of an applied voltage upon K_{eff} at the insulator-counter-electrode interface is somewhat different. Figure 15 shows the oxygen concentration at that interface based on the hypothesis that the catastrophe left the insulator essentially unchanged but enabled the counter-electrode to accept oxygen. Curve a shows the oxygen concentration prior to the catastrophe. This curve corresponds to a very high K_{eff} which agrees with the observed fact that no measurable current would flow in the reverse direction.

After the catastrophe, the oxygen concentration is given by curve b for the case where no voltage is applied. The junction is now quite diffuse, K_{eff} is much lower and current will flow if reverse voltage is applied. Application of a reverse voltage causes ion migration resulting in the oxygen concentration given by curve c. The barrier has now become less diffuse, K_{eff} is consequently increased and current flow decreases. Again, this is the voltage induced transient observed.

The changes in K_{eff} can readily be seen in Figure 16 which is a Schottky plot of the forward characteristic of Figure 11b. Line a shows the best fit to the outgoing characteristic up to about 20V. At this

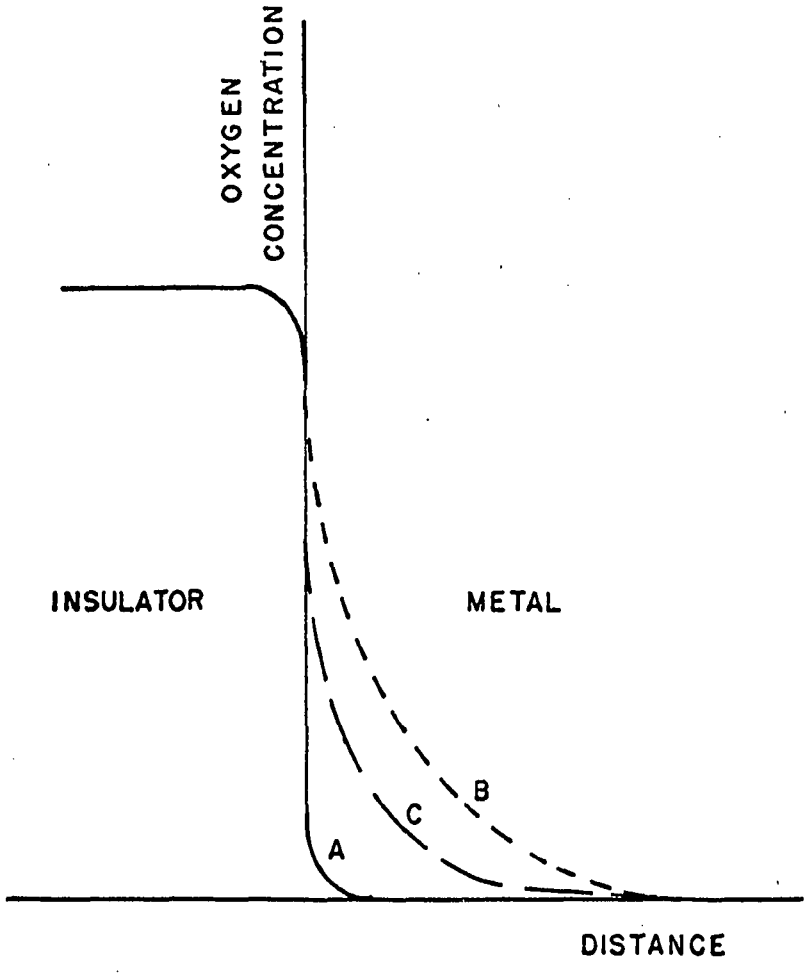

Figure 15. Oxygen concentration at the insulator-counter-electrode interface: (a) before catastrophe, (b) after catastrophe with no voltage applied, and (c) after catastrophe with voltage applied

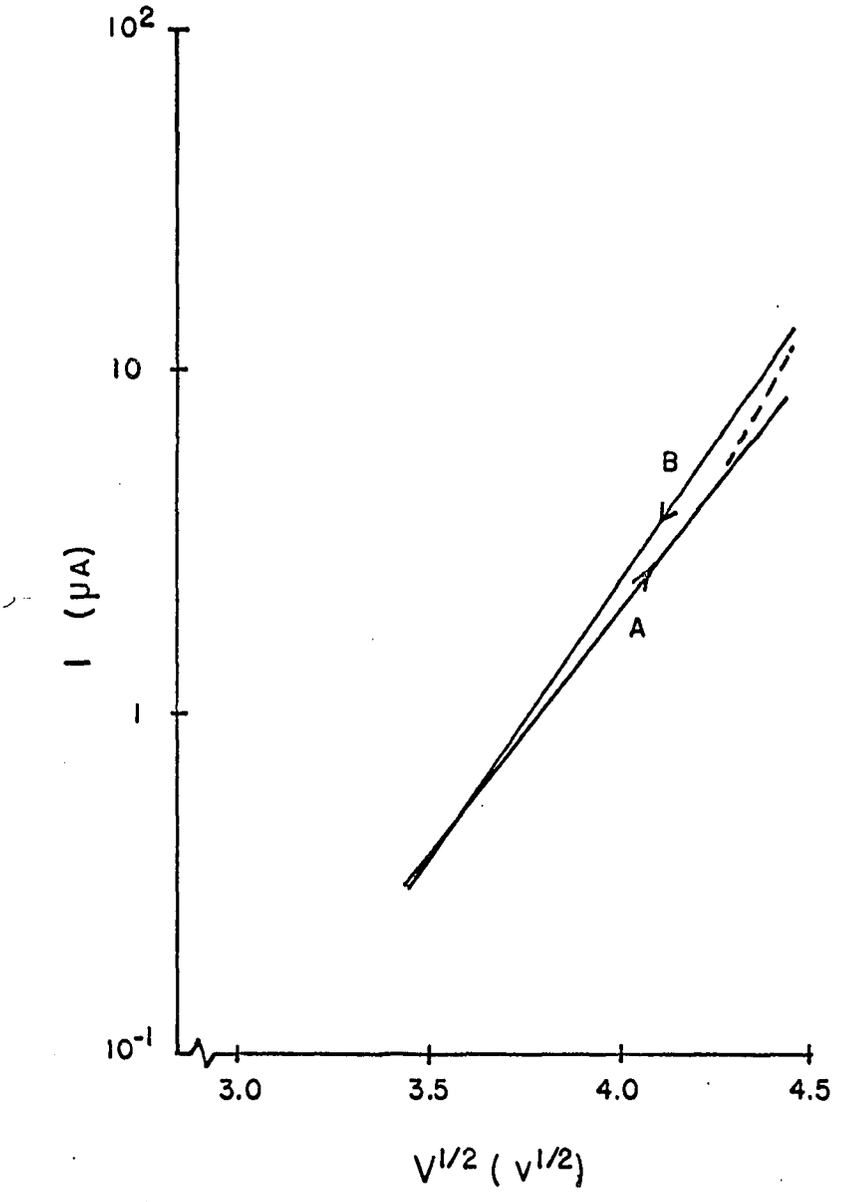

Figure 16. Schottky plot of forward characteristics of Figure 11b

point, a deviation from straight line behavior occurs as shown by the dashed line of somewhat greater slope. This deviation will be discussed later. Line b shows an excellent fit to the return characteristic.

For any straight line on a Schottky plot, K_{eff} is given by

$$K_{eff} = \frac{56200}{am^2} \qquad (10)$$

where a is the thickness of the barrier in angstroms and m is the slope of the line in units of volts $^{\frac{1}{2}}$/decade of current. (This equation is developed in the Appendix). This equation, using a thickness of 750 angstroms, shows that K_{eff} = 36.5 for line a and 26 for line b. These values are in the same range as the bulk value of K = 25 quoted by Hickmott (6) and their relative size agrees with the model just proposed.

The height of the potential barrier is given by

$$\phi = 0.0595\ (5.36 + mr - \log_{10} I_r) \qquad (11)$$

for a cell with an area of 2.2 mm^2 where r is the intercept in $V^{\frac{1}{2}}$ of the characteristic with the line $I = I_r$ and m is as previously defined. (This equation is developed in the Appendix). This equation shows that ϕ = 1.0 eV for line a and 1.06 eV for line b.

The aforementioned deviation from line a can probably be explained in terms of either rapid thermal effects, a change in the reflection coefficient in Richardson's equation or tunnelling into the insulator conduction band. It is felt that the first two explanations involve time constants which are too long to produce the deviation in a rapidly obtained characteristic. Tunnelling, however, can occur and indeed will occur if

the barrier is very thin. For the case of a relatively high K_{eff}, as in the outgoing characteristic, the barrier will be relatively thin. In the case of the return characteristic, line b, K_{eff} is lower, the barrier is thicker and the probability of the occurrence of tunnelling is much lower. Hence the return characteristic follows a straight line in an excellent fit.

In some respects, analysis of the reverse characteristics does not support the proposed model of the insulator-counter-electrode interface. The solid line of Figure 17 shows an excellent fit to the outgoing reverse characteristic of Figure 11b. The dots show the plotted points of the return characteristic. Any "best fit" straight line will have a slope which is greater than that of the outgoing characteristic, thereby indicating a lower K_{eff}, contrary to the model. The model does, however, predict that K_{eff} will be quite large on the return reverse characteristic and therefore tunnelling may be quite significant. Analysis of the outgoing characteristic using Equation 10 and Equation 11 indicate that $K_{eff} = 45$ and $\phi = 0.98$ eV.

Discussion of simple conduction

The model of a metal-insulator interface just presented is based upon Schottky emission over a barrier whose general shape is dependent upon the spatial variation of oxygen density. It assumes the mobility of oxygen ions under an applied field and neglects tunnel effects, at least in more diffuse barriers. The degree of diffusion of a barrier is related to an effective dielectric constant, K_{eff}, which is essentially a phenomenological parameter of the interface.

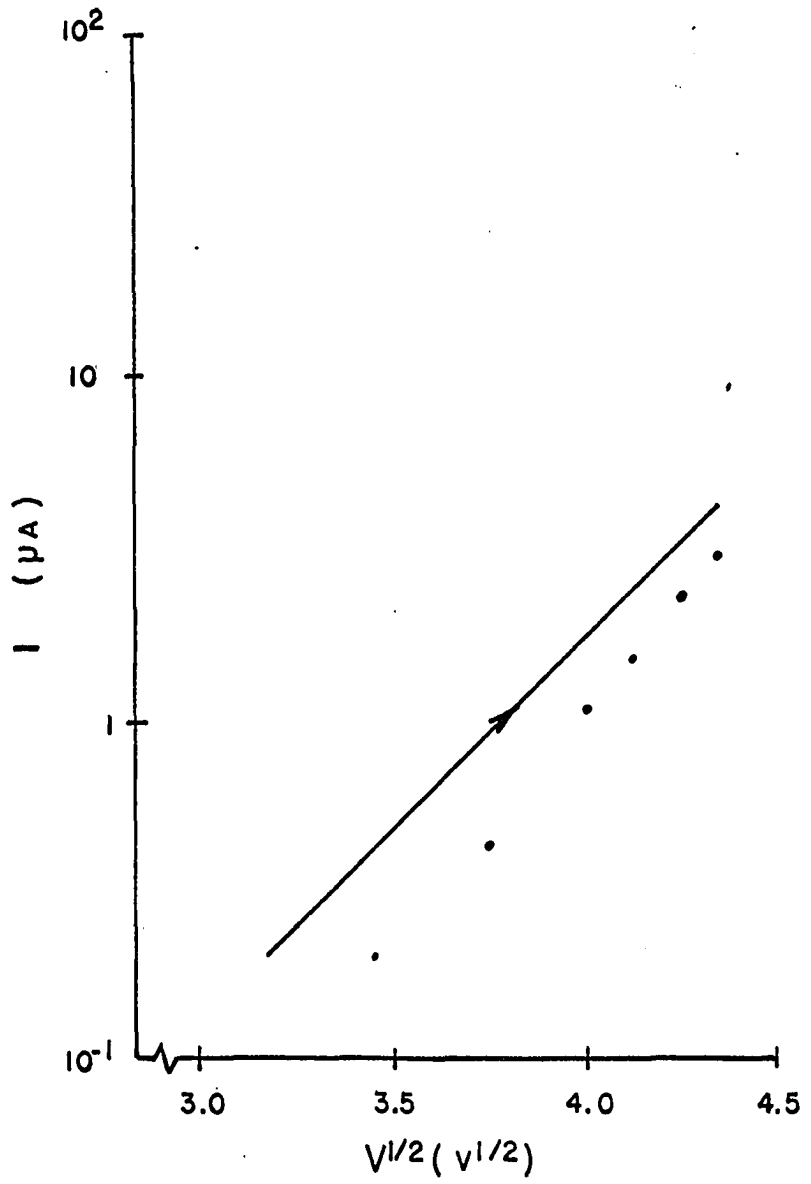

Figure 17. Schottky plot of reverse characteristics of Figure 11b

Correlation of the model with experimental data is good in a qualitative sense if one ascribes to the counter-electrode the ability to accept a limited quantity of oxygen and if one admits to tunnel effects in the thinner barriers. The value of K_{eff} determined experimentally are, in general, within one octave of 25, the bulk dielectric constant of Ta_2O_5. The height of the potential barrier is within 10% of 1 eV in all cases.

NEGATIVE RESISTANCE

Introduction

During the course of this investigation, a large number of the cells studies exhibited negative resistance properties. This phenomenon was first reported by Hickmott (6) in 1962 and was subsequently investigated in some detail by this same author (13). Most observations have been made on Al_2O_3 films, but others, including Ta_2O_5, have been used.

The negative resistance characteristics, examples of which are seen in Figure 18, are single valued in voltage. (It is interesting to note that precisely this same type of structure has exhibited negative resistance characteristics which are single valued in current (14, 15, 16). While predictability and reproductability of characteristics is rather poor, sufficient observations have been made to allow formulation of a few general comments.

Forming process

Prior to establishment of the negative resistance characteristic a generally erratic forming process must be completed. When voltage is first applied, the cell exhibits the exponential characteristic of simple conduction previously discussed.

In some cases this characteristic may be maintained through several cycles. At some point in the cycling, however, a partial breakdown occurs, characterized by a sudden increase of current, often on the order of two or three orders of magnitude. The characteristic is still generally exponential, however, and further cycling is required to establish negative resistance.

It is difficult to generalize concerning the nature of the characteristics obtained in this cycling because of rather significant differences in cells. It can be said, however, that marked hysteresis is generally noted and that a general trend toward an increase in current is present. These observations are in essential agreement with the forming process in Al_2O_3 described by Hickmott (13).

Data

Comparison of Figure 18a and Figure 18b demonstrates the difficulty encountered in generalizing the volt-ampere characteristics. One can only say that the characteristic most often encountered is nearly like that of Figure 18b with a voltage for maximum current, V_m, in the neighborhood of 4 volts. The Al_2O_3 cells observed had a V_m of about 3 volts and had characteristics similar in form to the Ta_2O_5 cells but were somewhat more erratic.

In most cells observed, the value of V_m on the outward leg of the characteristic was the same as that on the return leg. In some, however, a quite significant difference occurs. In one cell showing a particularly steep negative resistance portion, for instance, V_m was between 9 and 11 volts on the outward leg and between 5 and 7 volts on the return. The positive resistance portions of the outward and return characteristics were very nearly identical.

The positive resistance portions of the characteristics are generally exponential in form as shown in Figure 18. Normally, the positive resistance were somewhat erratic, showing quite rapid fluctuations in current at constant voltage. While fluctuations in the positive resistance portions

Figure 18. Two volt-ampere characteristics showing negative resistance

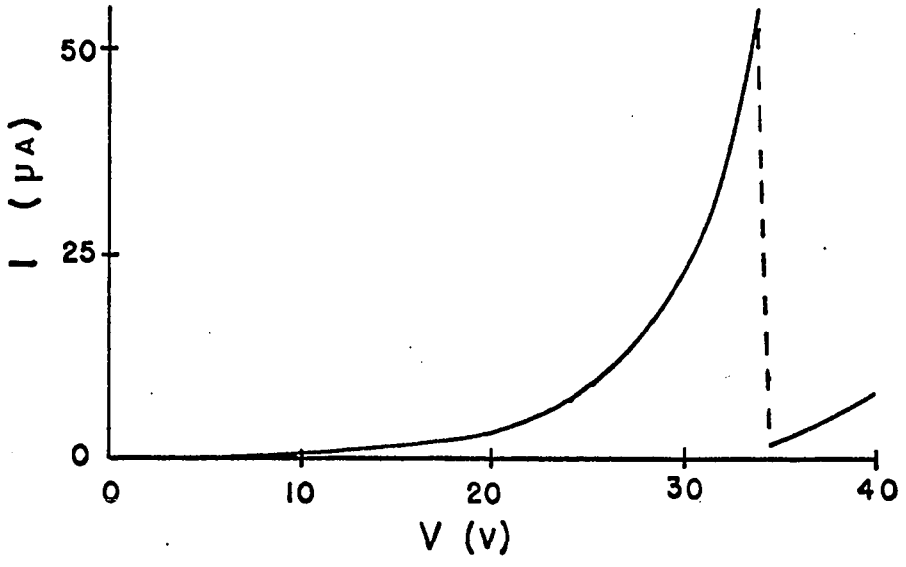

(A)

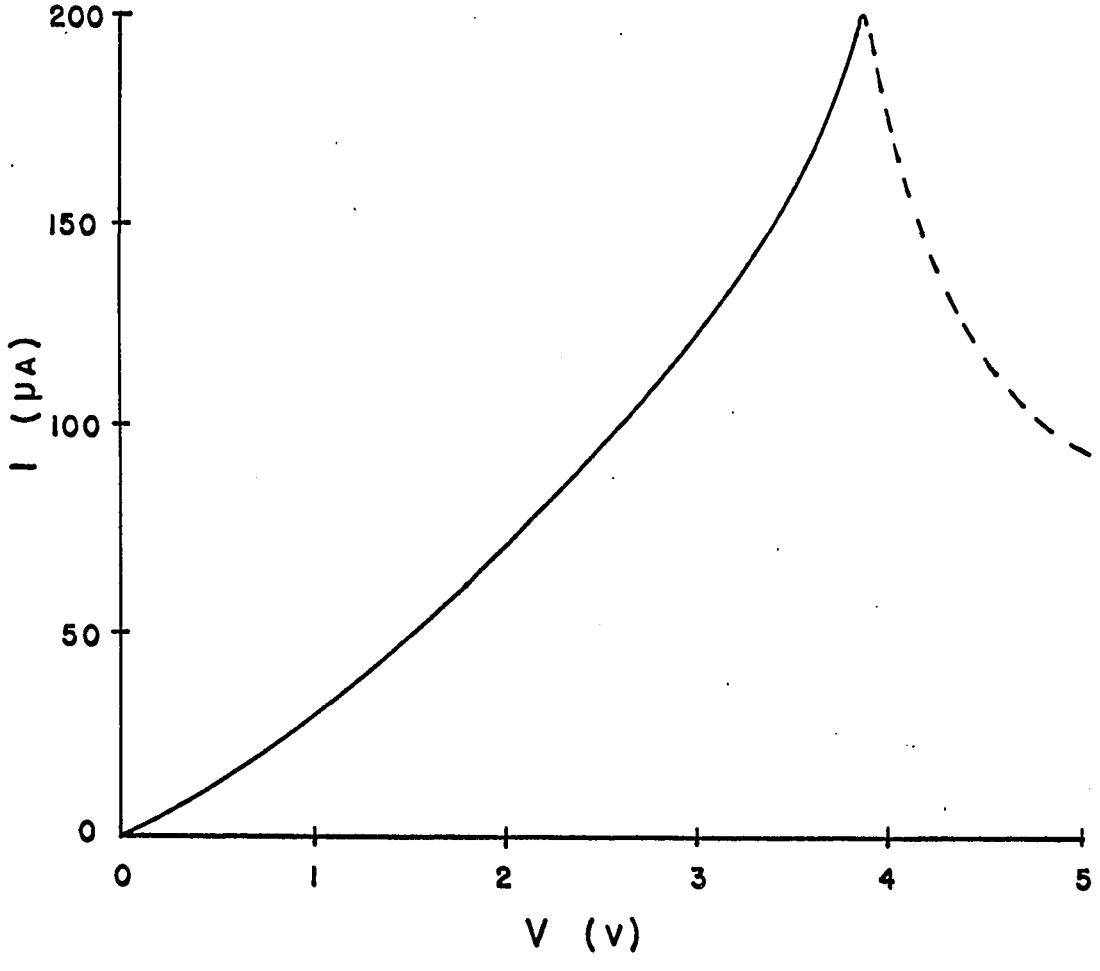

(B)

were rather small, those in the negative resistance portion were occasionally quite violent. This was particularly true in those characteristics having a relatively high negative resistance.

Analysis

The volt-ampere characteristic of Figure 18a is plotted in the Schottky plot of Figure 19. The characteristic shows an excellent fit to a straight line up to about 30 volts and then a tendency upward until V_m is reached. For voltages greater than V_m the characteristic is definitely curved with its slope decreasing as V increases. It is apparent that unadulterated Schottky emission is not solely responsible for the conduction current in either state of the cell.

It is interesting to analyze the Schottky plot of Figure 19 on a piecewise linear basis in the light of the modified Schottky emission model previously presented. By drawing several tangent lines and hypothesizing that these lines represent the conduction characteristics at the point of tangency the plot of ϕ versus $V^{\frac{1}{2}}$ of Figure 20 and the plot of K_{eff} versus $V^{\frac{1}{2}}$ of Figure 21 were obtained.

As seen in Figure 21, K_{eff} remains constant up to about 30 volts. As V is further increased, K_{eff} starts to decrease which would be expected if oxygen is allowed to migrate through the insulator. At the same time, ϕ starts to increase as seen in Figure 20. In the negative resistance portion of the characteristic K_{eff} and ϕ are not really defined, but from examination of Figure 21 and Figure 20 it is apparent that the trend established for V less than V_m must continue through this portion, i.e., K_{eff} continues to decrease and ϕ continues to increase as shown by the dashed

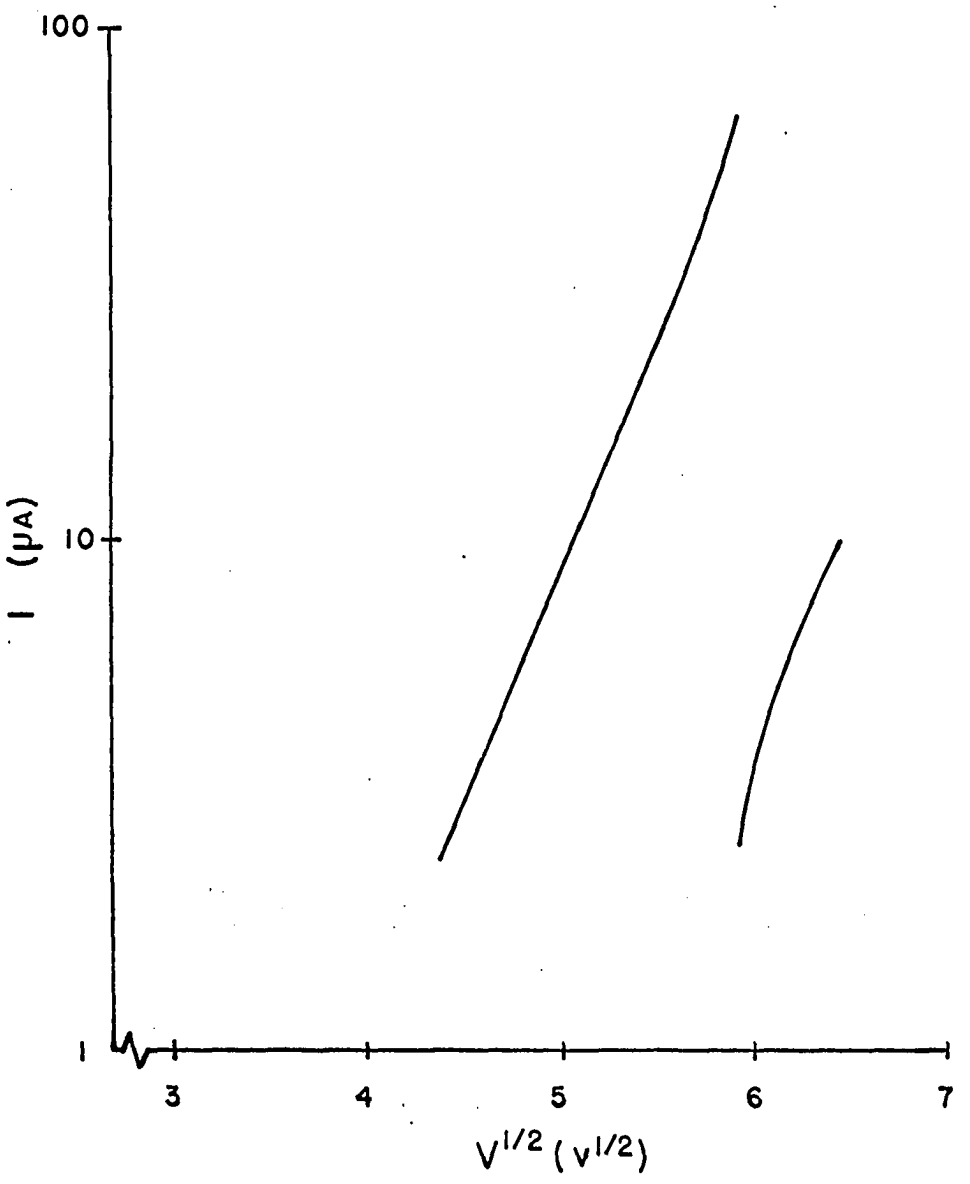

Figure 19. Schottky plot of volt-ampere characteristics showing negative resistance

Figure 20. Experimentally determined plot of potential barrier height versus square root of cell voltage

Figure 21. Experimentally determined plot of effective dielectric constant versus square root of cell voltage

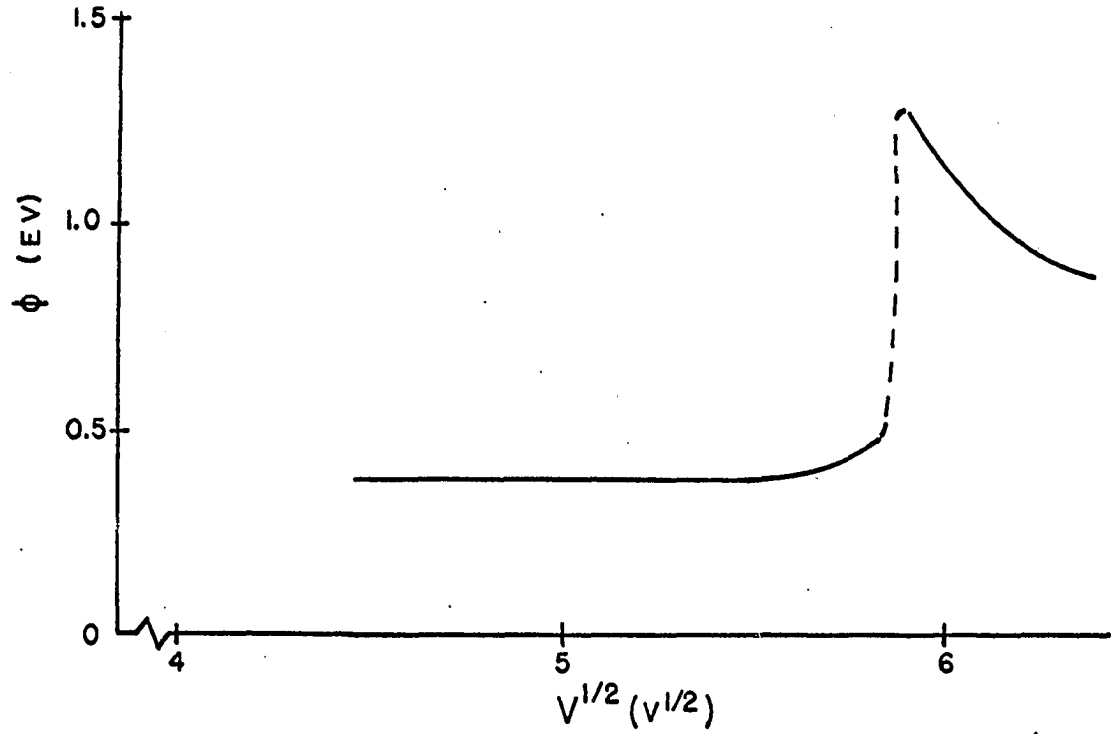
1.5
1.0
0.5
0
φ (EV)
4
5
6
V^1/2 (V^1/2)

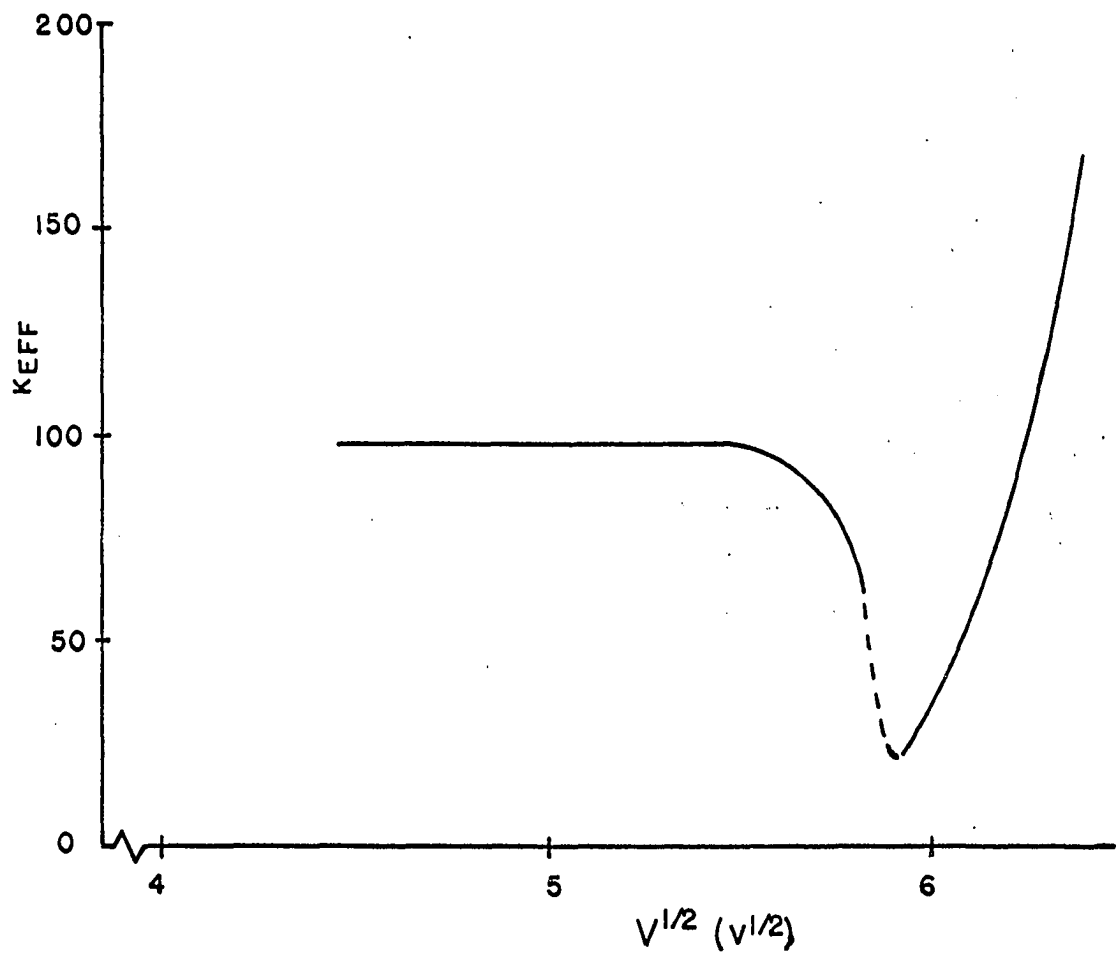
200
150
100
50
0
KEFF
4
5
6
V^1/2 (V^1/2)

lines. For voltages greater than those in the negative resistance portion, the trends reverse and ϕ decreases while K_{eff} increases.

Under the limitations of the Schottky emission hypothesis, one may conclude from the preceding paragraph that some process takes place in the negative resistance portion of the characteristic that results in a radical increase in ϕ with a small increase in voltage. Comparison of Figure 20 and Figure 21 further implies that this process does not take place until enabled by the characteristic decreases in K_{eff}. The long time constants involved in the voltage-induced increase of K_{eff} would dictate that the negative resistance characteristic could not be observed at high frequency. Hickmott (6) observed that this was indeed the case; a cell subjected to a 60 cps voltage with zero average showed no negative resistance in its volt-ampere characteristic. However, when this same cell was biased near the negative resistance region it exhibited switching times less than 0.5 microsecond. This indicates that the process responsible for the increase in ϕ may have quite a rapid response, but that for this process to take place some other process having a much slower response must have occurred.

The mechanics of the process responsible for the dramatic increase in ϕ is difficult to assess. Its rapid response leads one to conclude that it must be electronic in nature rather than ionic, which implies a change in space charge configuration in order to change ϕ. A severe lack of knowledge of the character of the insulator, not only at the interface but in the bulk film as well, precludes any detailed analysis. Certainly trapping at defect states in the insulator could play a role and, if one retains the Schottky emission concepts, velocity attenuation of the spec-

trum of emitted electrons could have a significant effect on the space charge configuration. Further, both of these actions could be dependent upon the shape of the potential barrier as characterized by K_{eff}.

Discussion of negative resistance phenomenon

At best, the analysis of negative resistance just presented is highly speculative. The good fit of the low voltage part of the characteristic to a straight line on the Schottky plot indicates that Schottky emission is probably dominant in that range. The hypothesis that it continues to dominate throughout the entire characteristic is, however, somewhat conjectural. It is supported by the observed response times of the cells and by the fact that K_{eff} tends in the right direction for voltage less than V_m. The initial value of ϕ (0.384 eV) seems quite low. However, the sudden increase in current in the forming process indicates that some very significant physical change has taken place in the insulator which could have the effect of lowering the barrier considerably. The changes in ϕ and K_{eff} for voltages beyond the negative resistance region is unexplained as is the mechanism responsible for the increase in ϕ in the neighborhood of V_m.

ELECTRON EMISSION

Introduction

When a metal-insulator-metal sandwich is biased in the forward direction (i.e., counter-electrode positive) electrons move across the insulator and are collected by the metal counter-electrode. If this counter-electrode is made sufficiently thin an electron possessing a non-zero kinetic energy has a definite probability of passing completely through it and being emitted into the medium beyond. Further, if this medium is vacuum, these electrons may be collected and/or utilized as desired.

This device and its use as a cold cathode was first proposed by Mead in 1960 (5). Later, Hickmott reported observing electron emission and compared the emission properties of several cells. (6, 17) An extensive study by Kanter and Feibelman using Al_2O_3 cells appeared in 1962.

Data

In this investigation, only Ta_2O_5 cells were used for electron emission studies. Most cells proved to be quite unstable in their emission properties, with the peak-to-peak amplitude of the instability being normally on the order of 25% of the average value of emitted current. A few cells, however, were sufficiently stable to allow measurements to be made to determine the energy of the emitted electrons.

The method of retarding potentials was used in the determination of electron energies. This method is based on the principle that an electron possessing a kinetic energy of E eV cannot pass a potential barrier of more than E volts. Therefore if one establishes a potential V_{ca} from the collector to the accelerator (collector negative), only those electrons

having energies greater than V_{ca} will reach the collector. Then if the resulting plot of collector current, I_c, versus V_{ca} is differentiated, one obtains a plot of the number of electrons per unit energy versus electron energy.

The principal difficulty encountered in the use of this method is the effect of space charge. This effect is illustrated in Figure 22 which is the potential diagram of the cell counter-electrode, the collector, and the intervening vacuum. Line a shows the potential with V_{ca} negative (i.e., collector positive). Space charge is present as evidenced by the curvature of the potential in the vacuum, but all emitted electrons reach the collector. Line b shows the situation existing when $V_{ca} = 0$. Now electrons which leave the emitting surface with energies less than ϕ_p eV will not pass the potential maximum and hence will not be received at the collector. This introduces error into the measurement since ideally with $V_{ca} = 0$, all electrons should be collected. Line c shows the potential with V_{ca} positive (i.e., collector negative). Now the peak of the space charge hump lies below the vacuum level of the collector and does not affect the number of electrons collected. Therefore, for low values of V_{ca}, one expects to find deviations from the expected behavior of the curve of I_c versus V_{ca}, but for high values of V_{ca} these deviations should disappear.

If one considers true thermionic emission where electron velocities follow a Maxwellian distribution one expects a plot of current versus retarding potential like that shown in Figure 23. If space charge were not present, the volt-ampere characteristic would follow the solid line. The presence of space charge modifies this characteristic in the vicinity

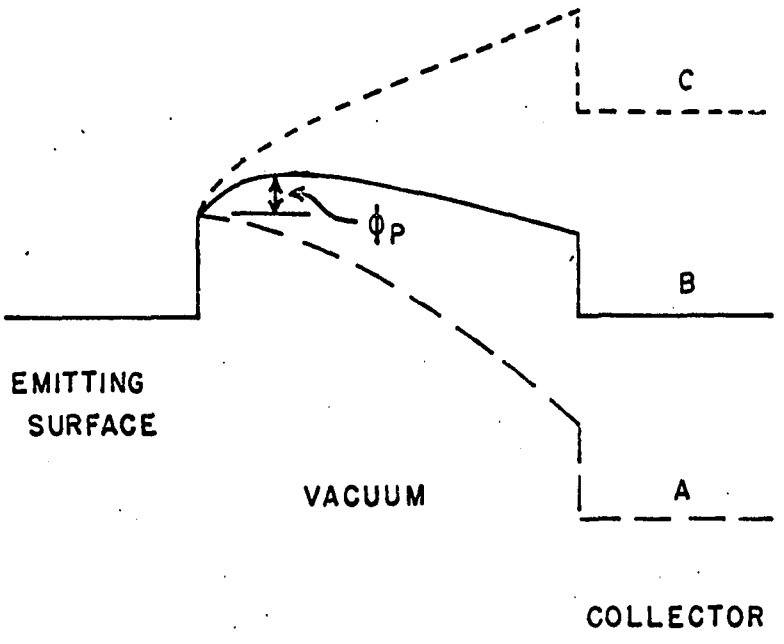

Figure 22. Potential diagram of an emitting surface, a collector and the intervening vacuum

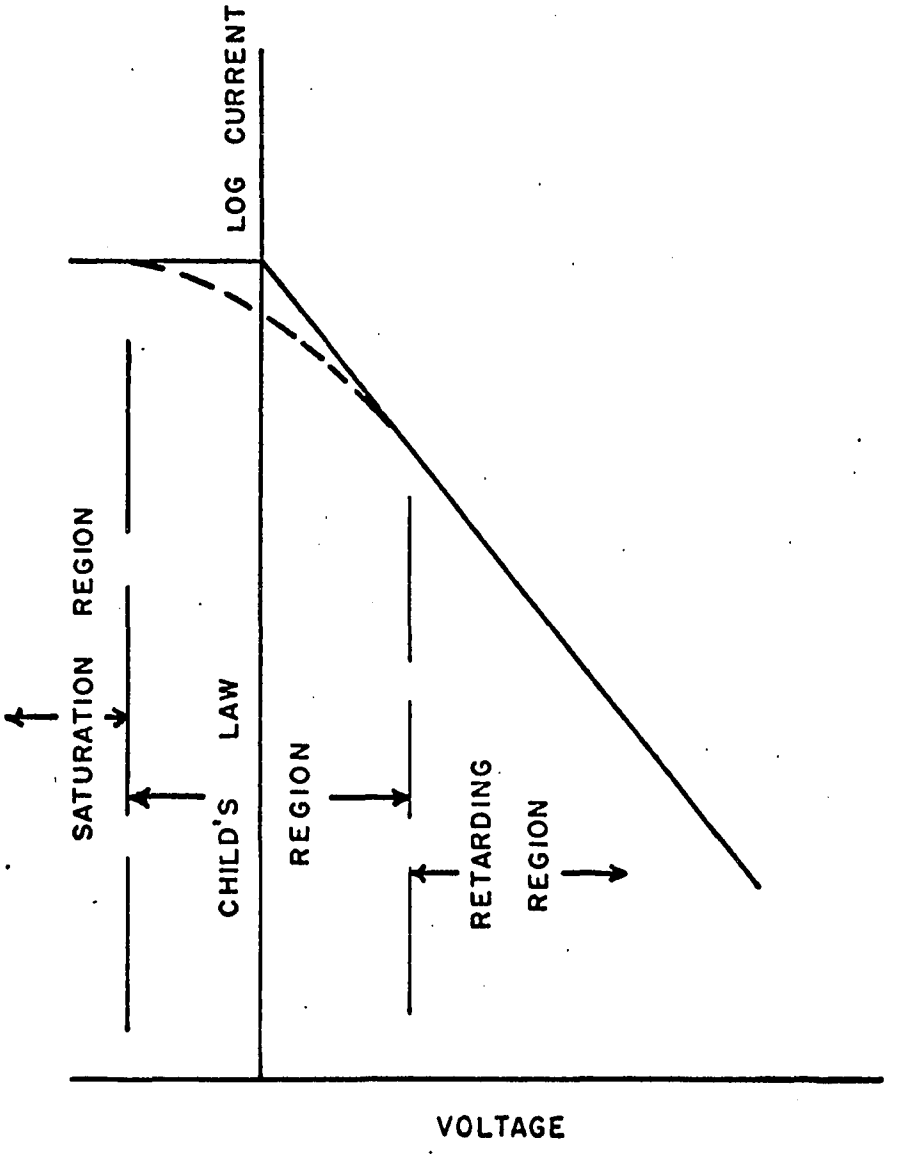

Figure 23. Logarithm of current versus retarding voltage for a thermionically emitted current - theoretical

of V = 0 as shown by the dashed line. The well-known Child's law or 3/2 power law is in effect in this region.

Figure 24 shows an experimentally determined plot of collector current versus retarding potential on a linear scale. The cell voltage V_{ea} was 25 volts. Note that there is a significant decrease in current for low negative values of V_{ca} indicating the presence of space charge effects. The same curve has been replotted in Figure 25 but with current plotted on a logarithmic scale. Comparison of Figure 25 and Figure 23 indicate that space charge effects become negligible for V_{ca} greater than about 3 volts. Between V_{ca} = 3 volts and V_{ca} = 13 volts the characteristics are what one would expect if the emitted electrons had a Maxwellian energy distribution. Above 13 volts the current is smaller than that predicted on this basis. This indicates that the higher velocity electrons are not present. No detectable current flowed for V_{ca} greater than 21 volts.

The plot of number of electrons per unit energy versus electron energy of Figure 26 was determined by mechanical differentiation of the characteristic of Figure 24. For voltages less than 3 volts the curve has been omitted since space charge effects have limited its accuracy.

Analysis

A simplified potential diagram of a metal-insulator-metal cell, a metal collector and the intervening vacuum is shown in Figure 27. By Schottky's theory any electrons having energies greater than ϕ_1 inside the emitter will, upon striking the emitter-insulator interface, pass into the insulator. By the simplest consideration, any electron so injected will be accelerated through the insulator and, in the absence of any loss

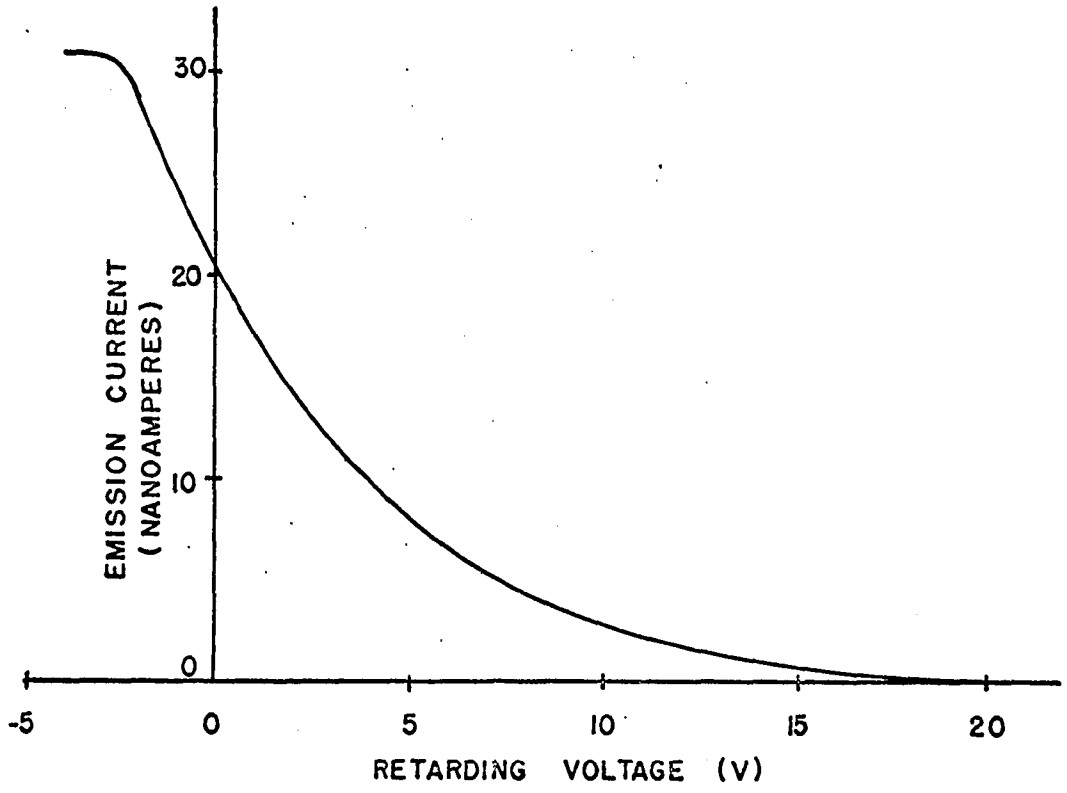

Figure 24. Emission current versus retarding potential - experimental

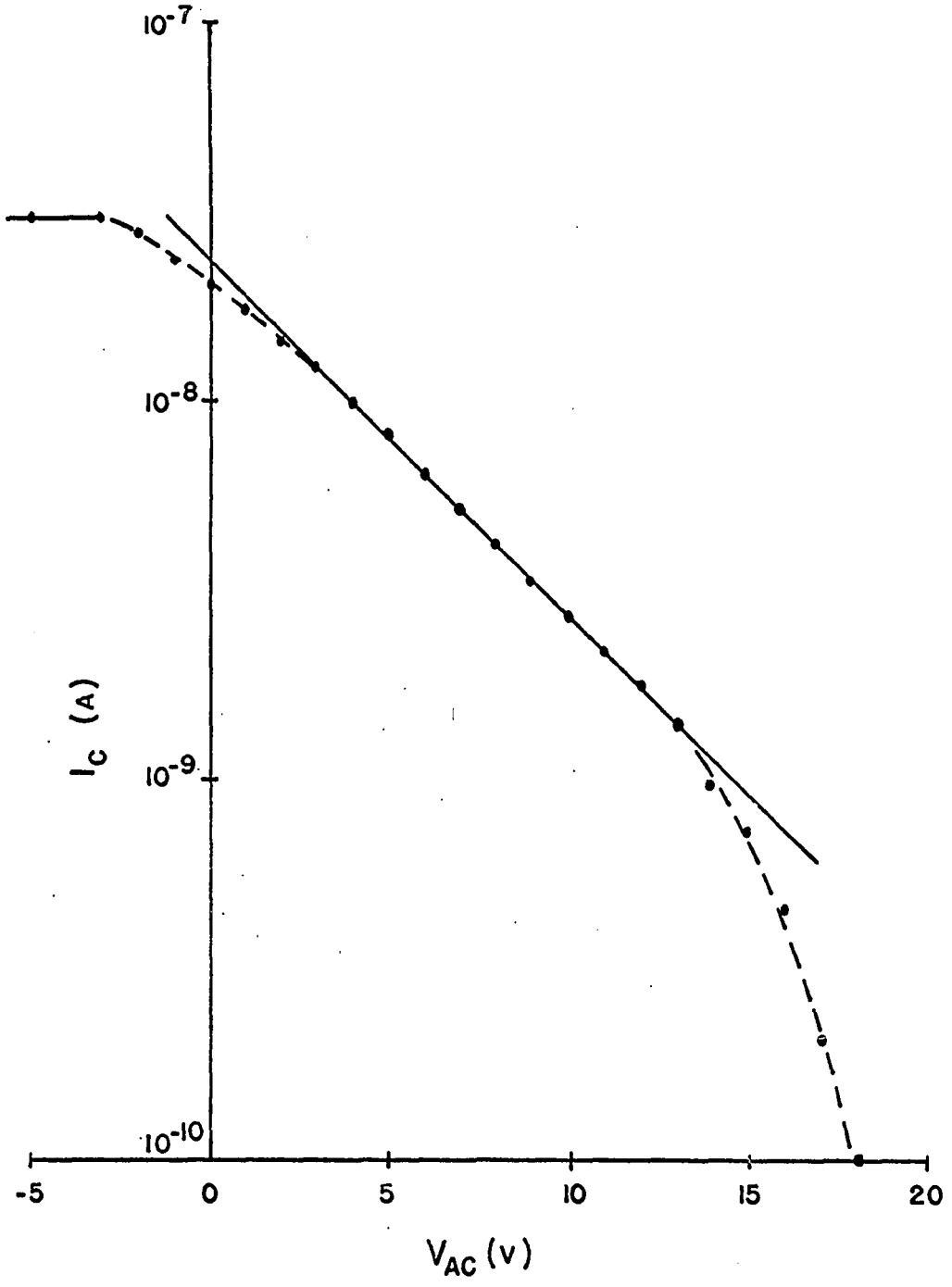

Figure 25. Logarithm of emission current versus retarding potential - experimental

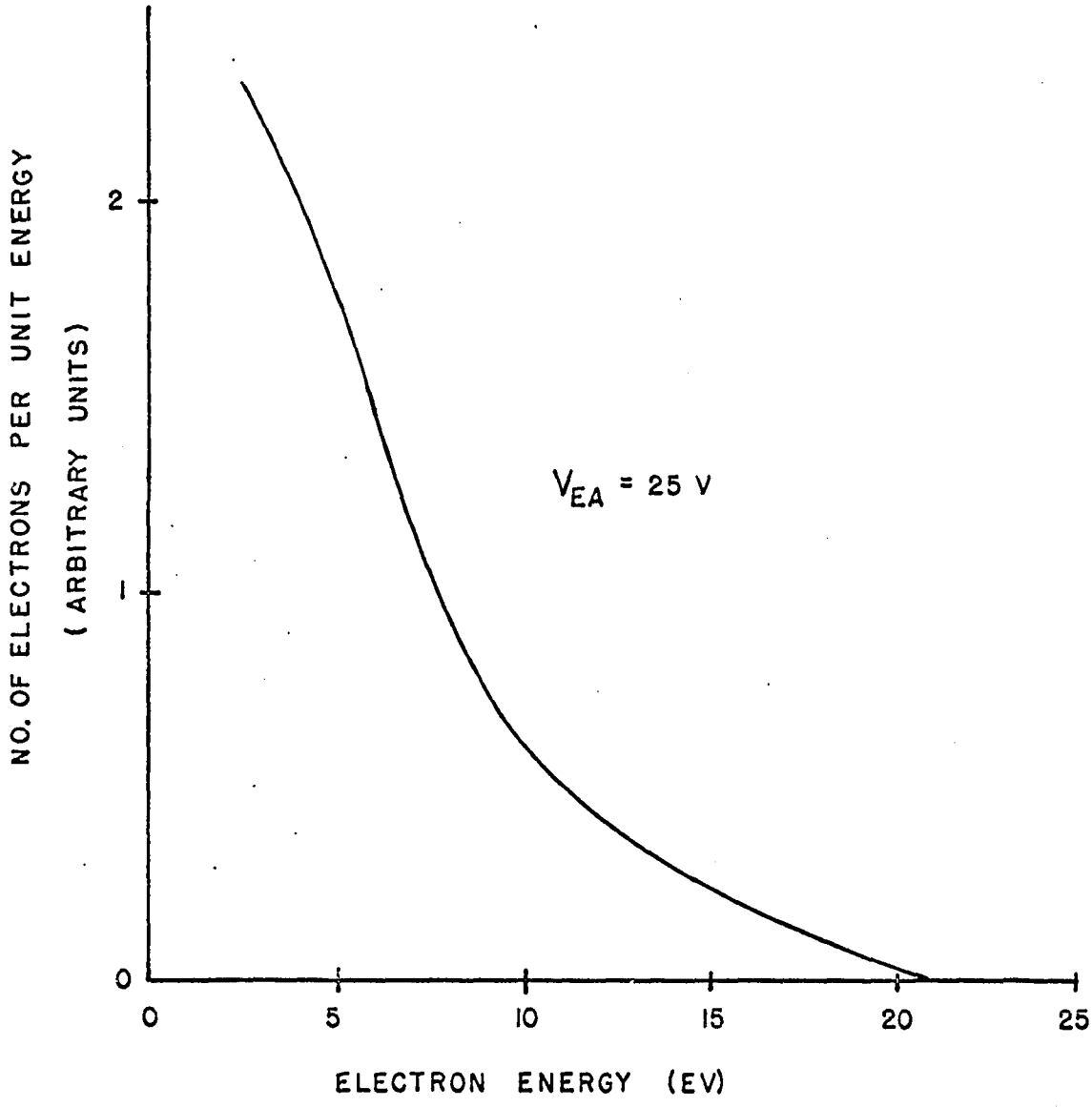

Figure 26. Experimentally determined energy spectrum of electrons emitted from a Ta_2O_5 cell

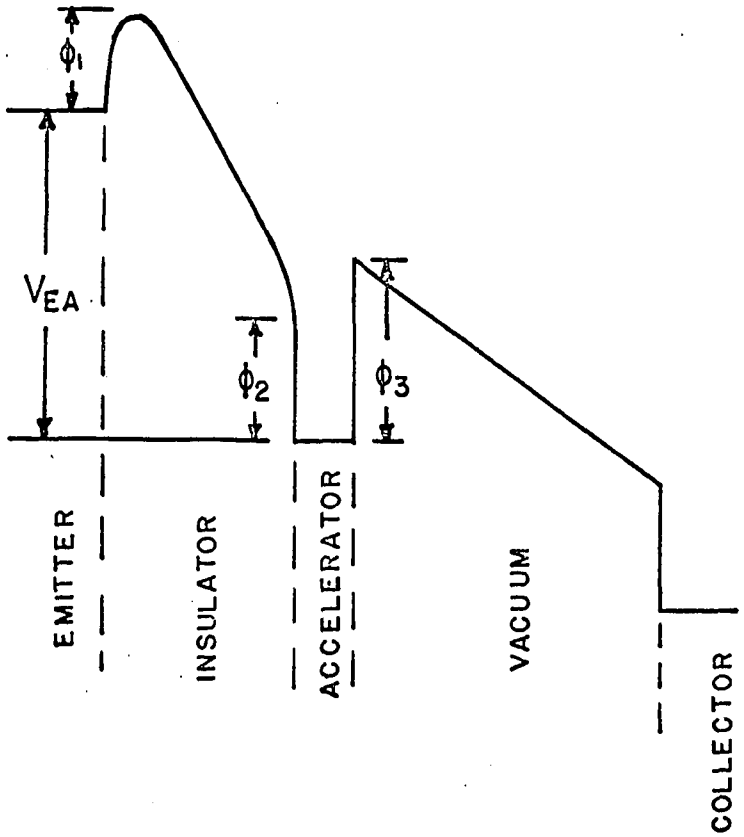

Figure 27. Potential diagram of a cell, a collector and the intervening vacuum

mechanisms, gain kinetic energy equal to eV_{ea} eV. When it strikes the insulator-accelerator interface it further gains energy and, passing through the accelerator, is emitted into vacuum with a kinetic energy equal to $e(V_{ea} - \phi_3)$ plus the energy that it originally possessed inside the emitter. This simple model predicts an energy distribution in the vacuum which is identical to that in the insulator near the emitter-insulator interface except that it is shifted along the energy axis by an amount $e(V_{ea} - \phi_3)$. This, of course, is not what is observed.

Instead, the maximum energy observed is very near $e(V_{ea} - \phi_3)$ although it must be pointed out that current measurement in this range is very difficult. Further, the total emitted current is 4 to 6 orders of magnitude below the total current transmitted through the insulator. If losses in the metal are considered to be small (Mead reports an attenuation length for Au of 100 angstroms) most of the electrons which enter the accelerator must have energies less than $e\phi_3$ (about 4.8 eV for Au). It appears, then, that substantial losses must occur in the insulator itself and that these losses are the limiting factor in the device.

Discussion of electron emission phenomenon

The rather large instabilities found in the electron emission currents from the cells studied make an accurate, detailed investigation of this phenomenon in Ta_2O_5 cells quite difficult. It was possible, however, to determine the electron energy spectrum of the emission current for electron energies greater than about 3eV. No electrons were detected which had energies greater than that given by the accelerating potential minus the work function of Au.

No emission studies were conducted on Al_2O_3 cells, but the stable performance of these cells reported in the literature indicate that they would be superior to those made with Ta_2O_5.

CONCLUSION

The preceeding pages have presented a series of observations on the conduction properties of tantalum oxide films. The characteristics of simple conduction, the phenomenon of negative resistance and the characteristics of electron emission have all been treated to varying degrees.

In the area of simple conduction many volt-ampere characteristics were obtained experimentally. In many cases, a good fit to Schottky characteristics was achieved, thus supporting the premise that the dominant conduction mechanism in thin insulating films is Schottky emission. A model for a metal-insulator interface based on the mobility of oxygen ions in the insulator was presented. This model, in which the degree of diffusion of the interface is expressed in terms of an effective dielectric constant, attempts to explain some of the peculiar conduction characteristics observed experimentally.

Under the hypotheses of this model, the barrier heights determined are within $\pm$ 10% of 1 eV and the values of effective dielectric constant range, in general, within one octave of 25, the bulk dielectric constant of tantalum oxide. The concept of barrier height is unchanged from Schottky's model but dielectric constant becomes essentially a phenomenological parameter of a given interface. The ability of this parameter to change in a biased interface is explained in terms of migration of ions in an applied field.

The phenomenon of negative resistance was observed in many cells. While the characteristics obtained were generally unstable, some very stable characteristics were obtained which allowed an analysis of the device in the light of the modified Schottky emission model. Under the

hypothesis that Schottky emission is the dominant conduction mechanism in the cell it was found that as voltage is increased the negative resistance region is preceded by a significant decrease in effective dielectric constant and followed by a significant increase. It was also found that the barrier height increases greatly as voltage is increased in the negative resistance region. Evidence is cited which indicates that the negative resistance phenomena may be due to an electronic process (characterized by an increase in barrier height) which can only take place after completion of some ionic process (characterized by a decrease in effective dielectric constant).

Electron emission currents were observed and the energy spectrum of the emitted electrons was determined. The retarding potential method was used in this determination of electron energies and as a result the presence of space charge effects detract seriously from the accuracy of the data below about 3 eV.

It was found that between 3 eV and 13 eV the energy spectrum was very nearly like that found in a thermionically emitted current. Above 13 eV the number of electrons per unit energy was found to be less than that expected in a thermionic current.

Certainly the study of conduction effects in thin insulating films is still in its infancy. The experimentalist in this field is faced with a seemingly endless array of variables, most of which are not thoroughly understood. The effects of anodizing time, anodizing current, anodizing voltage, impurity level, the many facets of the nature of the base metal, ambient temperature and pressure, the character of the counter-electrode,

etc., are very difficult to separate. Consequently, stated results are generalizations which attempt to summarize the average behavior of many cells while acknowledging the abnormalities that exist. Future experiments must involve very meticulous control and monitoring of each processing step to more nearly fix each known variable. This should lead to the discovery and understanding of variables which are as yet unrecognized and produce cells which are more uniform in their characteristics.

The engineering applications of the phenomena demonstrated by these cells are apparent. The negative resistance device, when a stable form is achieved, might find use as an amplifier, a switching device, a memory element, etc. Electron emission cells can be used as low-noise cold cathodes in vacuum tubes and for the injection of "hot" electrons into solid state devices. Some cells have exhibited rectifying properties and the use of cells as capacitors is well known. One can conceive of entire circuits built up using components made entirely of anodized metals.

It is hoped that the observations reported in these pages will contribute to the understanding of the mechanisms responsible for these phenomena and hasten the realization of stable, useful devices based thereon.

ACKNOWLEDGEMENTS

The author would like to thank Dr. A. A. Read of the Department of Electrical Engineering, Iowa State University, for his comments and encouragement during the pursuit of this investigation and for his criticism of this manuscript. He would also like to thank the Collins Radio Company, Cedar Rapids and particularly Dr. Frank Kottwitz of that company for their deposition of tantalum on the substrates supplied by the writer.

The author gratefully acknowledges the support given him by the United States Department of Health, Education and Welfare in the form of a National Defense Education Act Fellowship and by the Solid State Affiliates Program of Iowa State University.

Thanks are also due to Mrs. Regina Pluedeman for her most able and expeditious preparation of the final manuscript.

APPENDIX

In order to more readily evaluate the effective dielectric constant and the potential barrier of a cell whose volt-ampere characteristic is a straight line on a Schottky plot, expressions for these parameters in terms of the Schottky plot perameters will be derived. These expressions will also give some intuitive grasp of the significance of the slope and intercepts of the straight-line characteristic.

Consider the straight-line characteristic on the Schottky plot of Figure A1. Its equation is given by

$$\log_{10} I = \log_{10} I_r + m\,(V^{\frac{1}{2}} - r) \tag{A1}$$

or

$$.434 \log_e I = \log_{10} I_r - mr + mV^{\frac{1}{2}} \tag{A2}$$

where m, r, and I_r are defined in Figure A1.

Taking the antilogarithm of both sides, one obtains

$$I = e^{\frac{1}{.434}\,[\log_{10} I_r - mr]}\; e^{\frac{1}{.434}\,mV^{\frac{1}{2}}} \tag{A3}$$

If I is in amperes and the cell under investigation has a cross-sectional area, c, in cm^2 the equation becomes

$$I = \frac{1}{c} \exp\left[\frac{1}{.434}\,(\log_{10} I_r - mr)\right] \exp\left[\frac{1}{.434}\,mV^{\frac{1}{2}}\right] \tag{A4}$$

where I is now in a/cm^2.

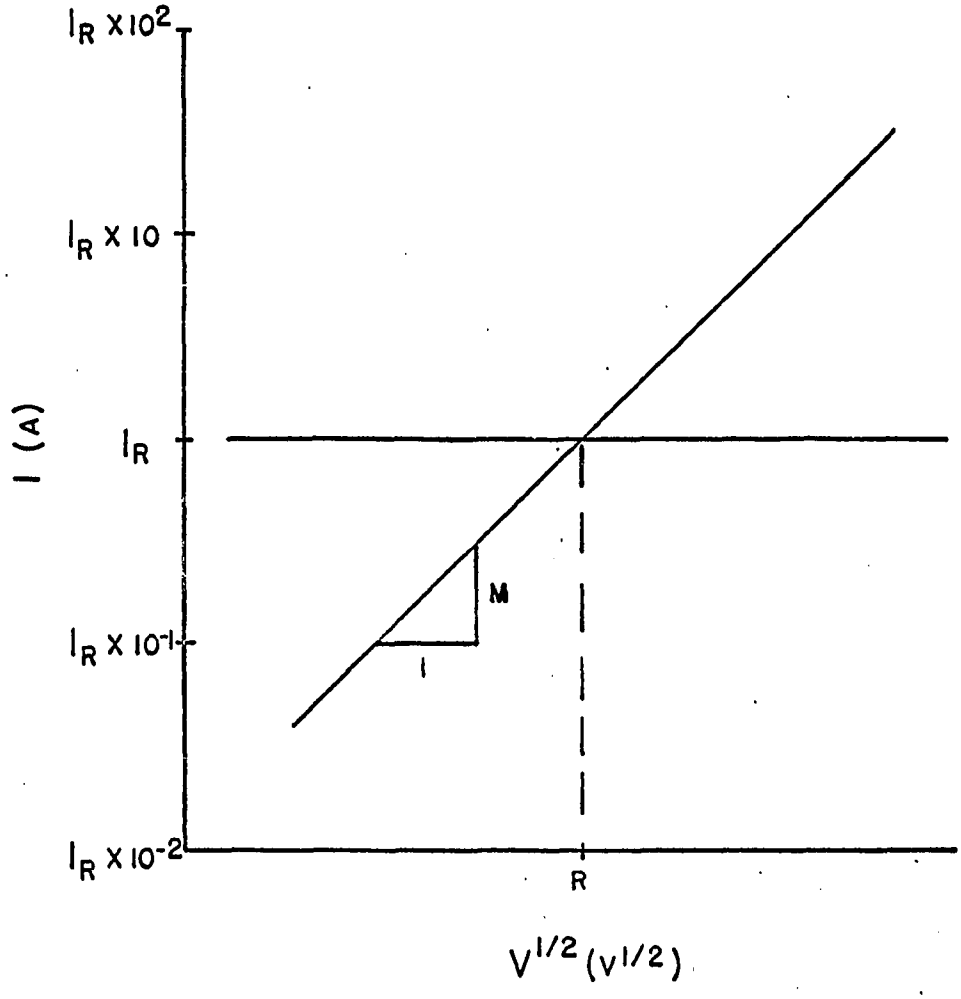

Figure A1. Generalized Schottky plot

Equation A4 is now the familiar form of Schottky's equation

$$I = AT^2 \exp(-\ /kT) \exp[(1/kT)(e^3/K\ \epsilon_o\ a)^{\frac{1}{2}}\ V^{\frac{1}{2}}] \qquad (A5)$$

where A is the Richardson constant (120 a/cm^2 ^oC), T is the absolute temperature, is the height of the potential barrier, k is the Boltzmann constant, e is the electronic charge, K is the dielectric constant of the insulator, ϵ_o is the permittivity of free space, and a is the insulator thickness. Equation corresponding terms yields

$$\frac{1}{C} \exp\left[\frac{1}{.434}\ (\log_{10} I_r - mr)\right] = AT^2 \exp(-\phi\ /kT) \qquad (A6)$$

and

$$\frac{1}{.434}\ m = (1/kT)(e^3/K\ \epsilon_o\ a)^{\frac{1}{2}} \qquad (A7)$$

Taking the logarithm of Equation A6 gives

$$\frac{1}{.434}\ (\log_{10} I_r - mr) - \log_e C = \log_e AT^2 - \phi\ /kT \qquad (A8)$$

$$\phi = kT\ [\ \log_e AT^2 + \log_e C - \frac{1}{.434}\ (\log_{10} I_r - mr)\ ] \qquad (A9)$$

At T = 300^{o}K, kT = 0.025 and $AT^2 = 1.08 \times 10^7$ so that

$$\phi = 0.0595\ [\ 7.04 + .434 \log_e C - \log_{10} I_r + mr\ ]\ eV \qquad (A10)$$

In the cell normally considered in these experiments C = 2.2×10^{-2} cm^2 and in this case

$$\phi = 0.0595\ [5.36 - \log_{10} I_r + mr\ ]\ \text{eV} \qquad \text{(A11)}$$

Note that if I_r is taken as 1 μa, 1 ma, 10 μa, etc., that $\log_{10} I_r$ is readily obtained.

Now squaring both sides of Equation A7 yields

$$\left(\frac{m}{.434} \right)^2 = \left(\frac{1}{kT} \right)^2 e^3 / K \varepsilon_o a \qquad \text{(A12)}$$

$$K = \frac{1}{am^2} \left(\frac{.434}{kT} \right)^2 \frac{e^3}{\varepsilon_o}$$

$$K = \frac{56{,}200}{am^2} \qquad \text{(A13)}$$

where a is in angstroms.

In the case of the cells studied in these experiments a = 750 angstroms and

$$K = \frac{75}{m^2} \qquad \text{(A14)}$$

LITERATURE CITED

1. Young, L. Anodic oxide films. New York, N. Y., Academic Press, Inc. 1961.

2. Kanter, H. and Feibelman, W. A. Electron emission from thin Al-Al_2O_3-Au structures. Journal of Applied Physics 33:3580. 1962.

3. Sommerfeld, A. and Bethe, H. Elektronentheorie der Metalle Handbuch der Physik 24:333. 1933.

4. Holm, R. and Kirschstein, B. Uber den Widerstand dunster Fremdschichten in Metalkontakten Zeitschrift für Technische Physik 16:488. 1935.

5. Mead, C. A. The tunnel emission amplifier. Proceedings of the Institute of Radio Engineers 48:359. 1960.

6. Hickmott, T. W. Negative resistance in thin anodic oxide films. Journal of Applied Physics 33:2669. 1962.

7. Kittel, C. Introduction to solid state physics. New York, N. Y., John Wiley and Sons, Inc. 1953.

8. Simmons, J. G. Electric tunnel effect between dissimilar electrodes. Journal of Applied Physics 34:2581. 1963.

9. Fisher, J. C. and Giaever, I. Tunnelling through thin insulating layers. Journal of Applied Physics 32:172. 1961.

10. Pollack, S. R. and Morris, C. E. Electron tunnelling through assymetric films of Al_2O_3. Journal of Applied Physics 35:1503. 1964.

11. Heil, H. Bulletin of the American Physical Society 7:327. 1962.

12. Standley, C. L. and Maissel, L. I. Some observations on conduction through thin tantalum oxide films. Journal of Applied Physics 35:1530. 1964.

13. Hickmott, T. W. Impurity conduction in thin oxide films. Journal of Applied Physics 35:2118. 1964.

14. Geppert, D. V. A new negative resistance device. Proceedings of the Institute of Electrical and Electronics Engineers 51:223. 1963.

15. Kallman, H. E. The assistor, a component with bipolar negative resistance. Proceedings of the Institute of Radio Engineers 50:2139. 1962.

16. Feigel, L. D. Negative resistance effects in thin titanium oxide films. Unpublished M.S. thesis. Ames, Iowa. Library, Iowa State University of Science and Technology. 1963.

17. Hickmott, T. W. Anomalous transmission of low energy electrons through thin metal films. Journal of Applied Physics 34:1569. 1963.